รายงานวิจัยฉบับสมบูรณ์

การสังเคราะห์ ศึกษาโครงสร้าง และคุณสมบัติในการยับยั้งจุลชีพของสารประกอบของโลหะรูทีเนียม(II) กับลิแกนด์ p-cymeme และ azo-imine

Synthesis, Characterization, Photo-physical properties, Electrochemistry and Antimicrobial Activity of Ruthenium(II) Complexes with p-Cymene and Azo-Imine Ligands

ผู้ช่วยศาสตราจารย์ ดร.นรารักษ์ หลีสกุล

โครงการวิจัยนี้ได้รับทุนสนับสนุนจากเงินรายได้มหาวิทยาลัยสงขลานครินทร์
ประจำปีงบประมาณ 2556
รหัสโครงการ SCI560355S

กิตติกรรมประกาศ

โครงการวิจัยนี้ได้รับสนับสนุนจากทุนเงินรายได้ มหาวิทยาสงขลานครินทร์ สัญญาเลขที่ SCI560355S ผู้วิจัยขอขอบคุณทางมหาวิทยาลัยในการสนับสนุนเงินทุนในการทำงานวิจัยเรื่องนี้ รวมถึงขอขอบคุณภาควิชาเคมี คณะวิทยาศาสตร์ มหาวิทยาลัยสงขลานครินทร์ ในการสนับสนุนสถานที่และเครื่องมือวิจัยที่เกี่ยวข้อง

นรารักษ์ หลีสกุล กุมภาพันธ์ 2560

บทคัดย่อ

สารประกอบแอรีนสองชนิด มีโครงสร้างที่เป็นส่วนสำคัญประกอบด้วยลิแกนด์ bis-diphosphinomethane (dppm) และลิแกนด์ *tert*-butylpyridine (tbp) ได้ถูกสังเคราะห์ขึ้น และศึกษาโครงสร้างด้วยเทคนิคการเลี้ยวเบนของรังสีเอกซ์ เทคนิคทางสเปกโตรสโกปีเทคนิคต่าง ๆ ได้แก่ ^{1}H-NMR ^{13}C-NMR 2D-NMR และ FTIR รวมถึงเทคนิคการวิเคราะห์หาปริมาณธาตุคาร์บอน ไฮโดรเจน และไนโตรเจน ซึ่งพบว่าเมื่อนำสารประกอบเชิงซ้อนที่สังเคราะห์ได้มาศึกษาฤทธิ์ในการเป็นสารต้านมะเร็งเต้านม โดยใช้เซลล์ไลน์เป็น MCF-7 และ HCC1937 ด้วยวิธี MTT assay พบว่าสารประกอบเชิงซ้อนของ [Ru(p-cymene)(dppm)Cl_2] แสดงการออกฤทธิ์ด้วยค่า IC50 ที่ดีกว่า (ต่ำกว่า) เมื่อเทียบกับสาร cisplatin ซึ่งใช้ทางการแพทย์ในปัจจุบัน โดยสามารถยับยั้งการเจริญเติบโตของเซลล์มะเร็งทั้งสองชนิดได้สูงกว่า cisplatin ถึง 16 เท่า นอกจากนี้สารประกอบเชิงซ้อน [Ru(p-cymene)(dppm)Cl_2] ยังมีฤทธิ์ในการยับยั้งเชื้อแบคทีเรีย *Staphylococcus aureus* ATCC25923 และเชื้อดื้อยา MRSA : methicillin resistant *Staphylococcus aureus* ด้วยค่า ด้วยค่า MIC/MBC 8/200 และ 32/128 ไมโครกรัมต่อมิลลิลิตร ตามลำดับ นอกจากนี้ยังแสดงการออกฤทธิ์ในการเป็นสารต้านเชื้อรา Cryptococcus neoformans ATCC90113 flucytosine-resistant, CN90113, ให้ค่า MIC/MBC 64/128 ไมโครกรัมต่อมิลลิลิตร อีกด้วย

Abstract

Two new arene compounds containing bis-diphosphinomethane (dppm) and *tert*-buytlpyridine (tbp) ligands as important components in Ruthenium(II) complexes were synthesized and characterized by X-ray crystallography, and spectroscopy of ^{1}H-NMR, ^{13}C-NMR, 2D-NMR, FTIR and CHN analysis. The synthesized complexes were evaluated in vitro as anticancer agents of human breast cancer cell lines, MCF-7 and HCC-1937, using the MTT assay. Both complexes showed an interesting behavior especially the compound of [Ru(dppm)(*p*-cymene) Cl_2]. It exhibited anticancer activity against both tested cell lines with greater IC50 values than cisplatin against all breast cancer cells. Both MCF-7 and HCC1937 cells exhibited 16-fold sensitivity to the [Ru(dppm)(*p*-cymene) Cl_2] compared to cisplatin. Furthermore, the [Ru(dppm)(*p*-cymene)Cl_2] complex significantly inhibited both *Staphylococcus aureus ATCC25923* ,and *MRSA = methicillin - resistant Staphylococcus aureus* with MIC/MBC values of 8/200 μg.mL^{-1} and 32/128 μg.mL^{-1}, respectively. In addition, it showed inhibition activity on *Cryptococcus neoformans* ATCC90113 flucytosine - resistant, CN90113, with an MIC/MBC value of 64/128 μg. mL^{-1}.

บทสรุปผู้บริหาร (Executive Summary)

บทนำ

สารประกอบออร์แกโนเมทัลลิกของโลหะทรานซิชันถูกนำมาใช้ประโยชน์ในงานทางการแพทย์และเภสัชวิทยาอย่างแพร่หลายมากขึ้นตั้งแต่มีการค้นพบว่าสาร cisplatin หรือ *cis*-$Pt(NH_3)_2Cl_2$ สามารถเป็นยาต้านมะเร็ง (Ronconi L. and Sadler P. J., 2007) แต่อย่างไรก็ตามการมีโลหะ Pt(II) อยู่ในโครงสร้างทำให้เกิดผลข้างเคียงโดยมีความเป็นพิษต่อเซลล์ปกติ ทำให้มีความพยายามในการค้นคว้าหาสารประกอบเชิงซ้อนหรือสารออร์แกโนเมทัลลิกอื่นที่สามารถออกฤทธิ์ทางชีวภาพได้โดยไม่ทำให้เกิดอันตราย หรือมีความเป็นพิษต่อเซลล์ปกติต่ำ สารประกอบเชิงซ้อนของโลหะรูทีเนียม (Ruthemium ทั้ง Ru(II) และ Ru(III)) จึงเป็นทางเลือกหนึ่งที่น่าสนใจเนื่องจากมีความเป็นพิษน้อย (Wang H., et al., 2012, Krstić M., et al., 2011) และสามารถจับกับ transferrin ซึ่งเป็นสารประกอบของธาตุเหล็ก ทำหน้าที่เป็นโปรตีนขนส่งเหล็กไปยังเนื้อเยื่อในร่างกาย และฮีโมโกลบินเพื่อสร้างเม็ดเลือดแดงได้ (Huxham L. A.., 2003) สารประกอบเชิงซ้อนของ *cis*- และ *trans*-$Ru(dmso)_4Cl_2$ เป็นตัวอย่างสารประกอบเชิงซ้อนชนิดหนึ่งที่สามารถนำมาใช้ประโยชน์เป็นสารต้านมะเร็ง (Huxham L. A., et al., 2003) โดยไม่ทำให้เกิดความเป็นพิษต่อเซลล์ปกติ นอกเหนือจากประโยชน์ในการเป็นสารต้านมะเร็งแล้ว สารประกอบเชิงซ้อนของโลหะรูทีเนียมยังเป็นสารออกฤทธิ์ในการต้านการเจริญเติบโตของเชื้อแบคทีเรียและเชื้อไวรัส (Prabhakaran R., et al., 2006, Sengupta P., et al., 2003, Thangadurai T. D., et al., 2010) อีกด้วย

จากการค้นคว้าบทความวิจัยที่เกี่ยวข้องพบว่า การมี arene ในโครงสร้างร่วมกับการมีลิแกนด์ชนิดอื่นเช่น ลิแกนด์ในหมู่อิมีน (imine, -N=C-C=N-) มักแสดงผลในการเป็นสารออกฤทธิ์ทางชีวภาพทั้งการเป็นสารต้านมะเร็ง (Henke H., et al., 2012, Harnif M., et al., 2010, Sipka S. G., et al., 2009, Renfrew A. K., et al., 2010) สารต้านเชื้อแบคทีเรีย (Beckford F., et al., 2011, Allardyce C. S., et al., 2003) และสารต้านเชื้อไวรัส (Allardyce C. S., et al., 2003) ซึ่งยังมีงานวิจัยน้อยมากที่ศึกษาความสามารถในการออกฤทธิ์ยับยั้งการเจริญเติบโตของจุลชีพ และการศึกษาการออกฤทธิ์ในการเป็นสารต้านมะเร็ง ของสารประกอบเชิงซ้อนของโลหะรูทีเนียมกับลิแกนด์ที่มีหมู่ฟังก์ชันทั้งหมู่ azo (-N=N-) และ imine (-N=C-C=N-) เป็นองค์ประกอบร่วม รวมถึงการใช้ลิแกนด์ที่มีฟอสฟอรัสเป็นหมู่ให้อิเล็กตรอน ในระบบที่มีลิแกนด์ p-cymene ร่วม ก็ยังไม่พบการตีพิมพ์ มีเพียงการศึกษาความสามารถในการออกฤทธิ์ทางชีวภาพของลิแกนด์ที่มีหมู่ฟังก์ชันใดฟังก์ชันหนึ่งของกลุ่มอิมีน (Albertin G., et al., 2011, Beckford F. A., et al., 2009) และกลุ่มเอโซ (Shridhar A. H., et al., 2012, Anitha C., et al., 2012) จึงคาดหวังว่างานวิจัยชิ้นนี้จะเป็นประโยชน์ต่องานด้านการออกแบบโครงสร้างเพื่อศึกษาความสามารถในการออกฤทธิ์ทางชีวภาพได้

ในงานวิจัยชิ้นนี้จึงเป็นการศึกษาโครงสร้างของสารประกอบเชิงซ้อนของโลหะรูทีเนียมที่สังเคราะห์ได้ด้วยเทคนิคทาง สเปกโทรสโกปี คุณสมบัติเชิงแสง คุณสมบัติทางไฟฟ้าเคมี รวมถึงการทดสอบการเป็นสารออกฤทธิ์ทางชีวภาพต่อเซลล์มะเร็งเต้านม MCF-7 และ HCC-1937 โดยใช้วิธี MTT assay เทียบกับการออกฤทธิ์ของ cisplatin ซึ่งเป็นสารมาตรฐานที่ใช้เป็นสารออกฤทธิ์ในยาต้านมะเร็งในปัจจุบัน ซึ่งพบว่ามีผลข้างเคียงจากการใช้ยาดังกล่าวต่อเซลล์ปกติมีมาก จึงนำมาสู่การพัฒนาสารอนินทรีย์ที่สามารถออกฤทธิ์ได้ดีแม้ใช้ในปริมาณต่ำ และไม่มีผลต่อเซลล์ในปริมาณดังกล่าวนั้น นอกจากนี้ยังศึกษาการเป็นสารต้านการเจริญเติบโตของเชื้อแบคทีเรีย ซึ่งใช้ตัวแทนเชื้อแบคทีเรียแกรมบวก ได้แก่ *Bacillus cereus* และ *Staphylococcus aureus* และแบคทีเรียแกรมลบ ได้แก่ *Escherichia coli* และ *Samonella* Typhimurium ซึ่งส่วนใหญ่เป็นเชื้อที่มักทำให้เกิดการติดเชื้อในระบบทางเดินอาหาร ส่งผลให้เกิดอาการท้องร่วงอย่างรุนแรงหรือเกิดภาวะอาหารเป็นพิษและลำไส้อักเสบ นอกจากนั้น *Staphylococcus aureus* ยังมีผลต่อการติดเชื้อที่ผิวหนังและระบบทางเดินหายใจ และบาดแผลที่เป็นฝีหนอง นอกจากนี้ยังมีการทดสอบกับเชื้อที่ดื้อยา ได้แก่ methicillin-resistant *Staphylococcus aureus* (MRSA) ซึ่งเชื้อต่าง ๆ เหล่านี้มักเป็นเชื้อพื้นฐานที่มีการตีพิมพ์เพื่อเทียบคุณสมบัติในการออกฤทธิ์เทียบกับยาบางชนิด เช่น เพนนิซิลิน (penicillin) และ เจนต้าไมซิน (gentamicin) เป็นต้น นอกจากนี้การทดสอบการออกฤทธิ์ทางชีวภาพยังศึกษาการออกฤทธิ์ต้านการเจริญเติบโตของเชื้อราก่อโรคบางชนิดที่มีผลต่อผู้ป่วยที่มีภูมิคุ้มกันบกพร่อง เช่น *Candida albicans* *Cryptococcus neoformans* และ *Penicillium marneffei* เป็นต้น

วัตถุประสงค์

1. เพื่อสังเคราะห์สารประกอบเชิงซ้อนชนิดใหม่ของ [Ru(p-cymene)(LL')Cl] เมื่อ LL' คือ bis-diphosphinomethane (dppm), *tert*-buytlpyridine (tbp) และไบเดนเทตลิแกนด์ *N,N'*-dialkylaminophenylazopyridine เมื่อ (alkyl = methyl และ ethyl)
2. เพื่อศึกษาโครงสร้าง สมบัติเชิงแสง และสมบัติทางไฟฟ้าเคมีของสารที่สังเคราะห์ได้
3. เพื่อศึกษาความสามารถในการออกฤทธิ์ของสารประกอบเชิงซ้อนที่สังเคราะห์ได้ต่อเชื้อแบคทีเรีย และเชื้อรา

สรุป

งานวิจัยชิ้นนี้ได้มีการสังเคราะห์สารประกอบเชิงซ้อนขึ้นจำนวน 4 สาร ได้แก่ [Ru(p-cymene)(dppm)Cl_2] (**1**) , [Ru(p-cymene)(tbp)Cl_2] (**2**) , [Ru(p-cymene)(dmazpy)Cl]Cl (**3**) และ [Ru(p-cymene)(deazpy)Cl]Cl (**4**) โดย p-cymene คือ ลิแกนด์ para-cymene, dppm คือ ลิแกนด์ bis-diphosphinomethane (dppm), tbp คือ ลิแกนด์ *tert*-buytlpyridine, dmazpy และ deazpy คือลิแกนด์

N,N'-dimethylaminophenylazopyridine และ *N,N'*-diethylaminophenylazopyridine ตามลำดับ โครงสร้างดังแสดงในรูปที่ 1

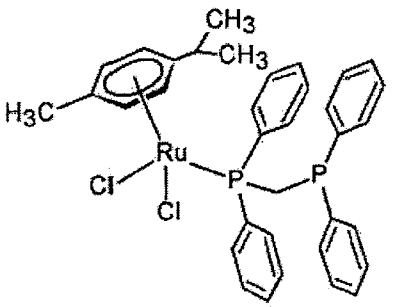

1

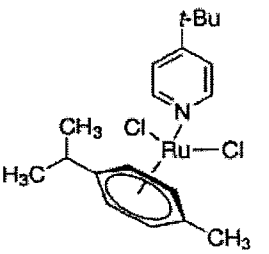

2

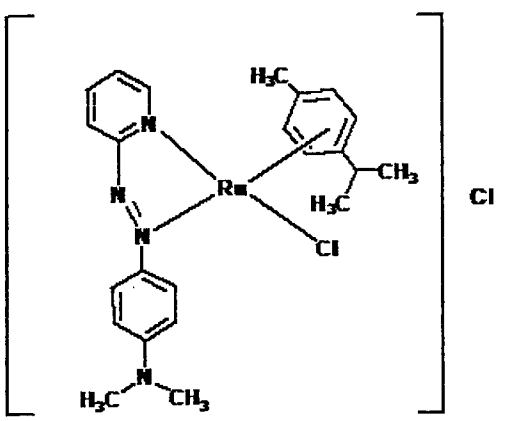

3

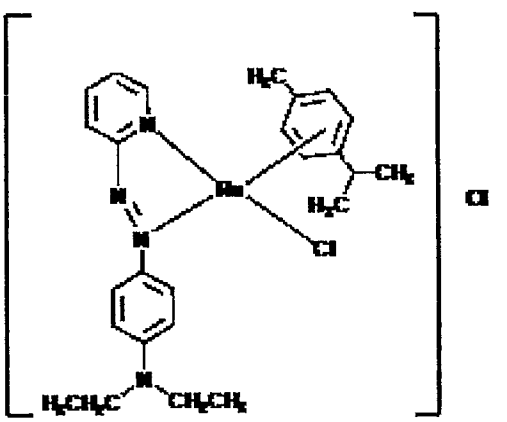

4

รูปที่ 1 โครงสร้างของสารประกอบเชิงซ้อนที่ศึกษา

พบว่าสารประกอบที่สังเคราะห์ได้ทั้งสี่ชนิดมีโครงสร้างเป็นรูปทรงเตตระฮีดรอลบิดเบี้ยว (distortet tetrahedral) โดยในกรณีของสารประกอบเชิงซ้อนที่ 1 นั้นแม้จะมีลักษณะเป็นลิแกนด์ไบเดนเทต (bidentate ligand) ที่ 1 โมเลกุล สามารถเกิดพันธะกับรูทีเนียม (II) ได้ 2 พันธะก็ตาม แต่ผลจากการศึกษาโครงสร้างพบว่าโมเลกุลของลิแกนด์ dppm เกิดพันธะในลักษณะโมโนเดนเทต (monodentate) และมีคลอโร (Cl) ลิแกนด์เป็นตัวดุลประจุทำให้โมเลกุลมีความเป็นกลาง ซึ่งแม้จะไม่ใช่รูปทรงที่แบนราบ แต่มีโอกาสที่คลอโรลิแกนด์ในโครงสร้างซึ่งเป็นลิแกนด์ที่ไม่ได้แข็งแรงนัก สามารถหลุดออกเพื่อให้สารประกอบเชิงซ้อนของรูทีเนียมสามารถเข้าไปจับกับคู่เบสของเซลล์มะเร็งได้ ในขณะที่สารประกอบเชิงซ้อนที่มีลิแกนด์ dmazpy และ deazpy ที่มีหมู่เอโซอิมีน เป็นหมู่ฟังก์ชันหลักนั้นพบว่าจากการศึกษาโครงสร้างด้วยเทคนิคทางสเปกโตรสโกปี พบว่าสารประกอบเชิงซ้อนที่สังเคราะห์ได้ลิแกนด์เกิดพันธะแบบไบเดนเทตสร้างวงคีเลตที่แข็งเรงขึ้นได้จึงทำให้โครงสร้างเป็นสารประกอบเชิงซ้อนประจุบวก

โดยสารประกอบเชิงซ้อนออกแบบโครงสร้างเพื่อศึกษานั้น ถือได้ว่าเป็นสารออร์แกโนเมทัลลิกที่มี p-cymene เป็นสารอะโรแมติกไฮโดรคาร์บอนที่ใช้อะตอมคาร์บอนในวงแหวนฟีนิล (phenyl) ยึดเหนี่ยวกับโลหะรูทีเนียมประจุ 2+ ผ่าน N อะตอมของวงแหวนพิริดีนและหมู่เอโซ และ P อะตอมของลิแกนด์ bis-diphosphinomethane (dppm) ซึ่งการมีโครงสร้างที่เป็นคีเลต และ/หรือการมีวงแหวนฟีนิลในโครงสร้าง ทำให้มีความเป็น lipophillic สูงขึ้น เอื้อต่อการแพร่ผ่านเซลล์เมมเบรนของเชื้อแบคทีเรียหรือเชื้อราได้ง่ายขึ้นตามทฤษฎี Tweedy chaltion (Venkatachalam G., et.al., 2005, Balasubramanian K. P., et. al., 2006) ทำให้มีแนวโน้มที่จะสามารถยับยั้งการเจริญเติบโตของจุลชีพได้ดี ซึ่งสารประกอบเชิงซ้อนทั้ง 4 ชนิดมีฤทธิ์ทางชีวภาพในการเป็นสารยับยั้งการเจริญเติบโตของเซลล์มะเร็ง โดยเฉพาะมะเร็งเต้านม โดยสารที่ให้การออกฤทธิ์สูงสุดคือ [Ru(p-cymene)(dppm)Cl_2] ให้การออกฤทธิ์ยับยั้งการเจริญเติบโตของเซลล์มะเร็งเต้านมได้มากกว่า cisplatin ถึง 16 เท่า (IC50 42.2 ± 8 สำหรับ MCF-7 และ 23.4 ± 7 สำหรบ HCC-1937) โดยได้วิเคราะห์ความเป็นพิษต่อเซลล์ปกติผ่านการทดสอบกับ Vero cells (African green monkey kidney) ด้วยวิธี Green Fluorescent Protein (GFP)-based assay พบว่าให้ค่า IC50 ที่ 19.94 ไมโครกรัมต่อมิลลิลิตร ซึ่งเป็นความเข้มข้นที่สูงกว่าค่า IC50 เมื่อทดสอบกับเซลล์มะเร็งเต้านม MCF-7 และ HCC-1937 (2.6 ± 0.2 และ 1.4 ± 0.3 ตามลำดับ)

และนอกจากนี้ [Ru(p-cymene)(dppm)Cl_2] ยังเป็นสารออกฤทธิ์ต้านการเจริญเติบโตของแบคทีเรียแกรมบวก *Staphylococcus aureus* และเชื้อดื้อยา methicillin - resistant *Staphylococcus aureus* (MRSA) ได้แต่ยังไม่ดีเท่ากับยาทางการค้า ซึ่งงานวิจัยชิ้นนี้ได้แบ่งการตีพิมพ์ผลงานออกเป็น 2 ผลงาน ผลงานแรกเป็นของ [Ru(p-cymene)(dppm)Cl_2] และ [Ru(p-cymene)(tbp)Cl_2] ซึ่งมีผลศึกษาโครงสร้างผลึกเดี่ยวจากเทคนิคการเลี้ยวเบนของรังสีเอกซ์แล้ว ทำให้ยืนยันโครงสร้างได้ชัดเจน และให้ผลในการออกฤทธิ์การเจริญเติบโตของเซลล์มะเร็งได้ดี จึงมีความโดดเด่นและความน่าสนใจเพียงพอที่จะตีพิมพ์ผลงานได้ก่อน อีกผลงานหนึ่งเป็นของสารประกอบเชิงซ้อนที่มีลิแกนด์ในกลุ่มเอโซอิมีนของสารประกอบเชิงซ้อน [Ru(p-cymene)(dmazpy)Cl]Cl และ [Ru(p-cymene)(deazpy)Cl]Cl ให้ค่าการยับยั้งเซลล์มะเร็งเต้านม MCF-7 ที่ความเข้มข้น 50 ไมโครกรัมต่อมิลลิลิตร สามารถยับยังได้ 98.31 และ 99.40 % ตามลำดับ

ภาคผนวก

Journal of Organometallic Chemistry 846 (2017) 242–250

Contents lists available at ScienceDirect

Journal of Organometallic Chemistry

journal homepage: www.elsevier.com/locate/jorganchem

Synthesis, X-ray structure of organometallic ruthenium (II) *p*-cymene complexes based on P- and N- donor ligands and their in vitro antibacterial and anticancer studies

Parichad Chuklin [a], Vachirawit Chalermpanaphan [a], Tidarat Nhukeaw [b], Saowanit Saithong [a], Kittipong Chainok [c], Sauwalak Phongpaichit [d], Adisorn Ratanaphan [b], Nararak Leesakul [a, *]

[a] Department of Chemistry and Center for Innovation in Chemistry, Faculty of Science, Prince of Songkla University, Hat Yai, Songkhla 90110, Thailand
[b] Department of Pharmaceutical Chemistry, Faculty of Pharmaceutical Sciences, Prince of Songkla University, Hat Yai, Songkhla 90112, Thailand
[c] Department of Physics, Faculty of Science and Technology, Thammasat University, Klong Luang, Pathumthani 12120, Thailand
[d] Natural Products Research Center and Department of Microbiology, Faculty of Science, Prince of Songkla University, Hat Yai, Songkhla 90110, Thailand

ARTICLE INFO

Article history:
Received 24 June 2016
Received in revised form
10 June 2017
Accepted 18 June 2017
Available online 19 June 2017

Keywords:
Antimicrobial activity
Anticancer activity
Ru(II)-Arene

ABSTRACT

Two new arene compounds containing bis-diphosphinomethane (dppm) and *tert*-butylpyridine (tbp) ligands as important components in ruthenium(II) complexes were synthesized and characterized by X-ray crystallography, and spectroscopy of ^{1}H NMR, ^{13}C NMR, 2D-NMR, FTIR and CHN analysis. The synthesized complexes were evaluated in vitro as anticancer agents of human breast cancer cell lines, MCF-7 and HCC1937, using the MTT assay. Both complexes showed an interesting behavior especially the compound of [Ru(*p*-cymene) (dppm)Cl_2]. It exhibited anticancer activity against both tested cell lines with greater IC_{50} values than cisplatin against all breast cancer cells. Both MCF-7 and HCC1937 cells exhibited 16-fold sensitivity to the [Ru(*p*-cymene)(dppm)Cl_2] compared to cisplatin. Furthermore, the [Ru(*p*-cymene)(dppm)Cl_2] complex significantly inhibited both *Staphylococcus aureus* ATCC25923 and MRSA = methicillin resistant *Staphylococcus aureus* with MIC/MBC values of 8/200 μg mL^{-1} and 32/128 μg mL^{-1}, respectively. In addition, it showed inhibition activity on *Cryptococcus neoformans* ATCC90113 flucytosine - resistant, CN90113, with an MIC/MBC value of 64/128 μg mL^{-1}.

1. Introduction

At the present time, some platinum drugs like cisplatin, carboplatin and oxaliplatin are commonly used in the treatment of numerous types of cancer cells [1]. Nevertheless, these kinds of drugs can cause side effects including dehydration, risk of infection, kidney toxicity and many other abnormalities [2]. Half sandwich ruthenium(II)-arene complexes have been widely investigated and challenged to develop their pharmaceutical potential as anti-cancer agents with lower toxicity to normal cells than platinum(II) complexes. Half-sandwich metallocenes are effectively used for medicinal applications. Various half sandwich organometallic (η^6-arene)-ruthenium (II) complexes with *p*-cymene ligands show promising anticancer behavior [3,4]. A distorted psuedo-tetrahedral structure coordinated with *p*-cymene to the ruthenium(II) center, like the typical "piano-stool" geometry, is of extensive interest. Other coordinated bonds normally occur with functional and chloro ligands. There exist several types of functional ligands with Nitrogen [5], Oxygen [6], Sulfur [7] and Phosphorus [8] donors. Most structures are designed to be ionic complexes soluble in water [9,10]. On the other hand, many neutral complexes exhibit promise as anticancer drugs [11,12] because they are kinetically stable, relatively lipophilic, and their metal atoms are in states of low oxidation [13]. Notable examples of anticancer compounds are ruthenium complexes consisting of diphosphine derivative ligands like 1,1-bis(diphenylphosphino) methane (dppm) and 4,5-bis(diphenylphosphino)-9,9-dimethylxanthene (Xantphos). Recently reported by Rodríguez-Bárzano and co-workers [14], they exhibited excellent IC_{50} values in nanomolar normoxic A2780 (human ovarian carcinoma) and HT-29 (human colon carcinoma) cell lines. Their reported complexes are both in

* Corresponding author. Tel.: 00 66 74 28 8421; fax: 00 66 74 55 8841.
E-mail address: nararak.le@psu.ac.th (N. Leesakul).

http://dx.doi.org/10.1016/j.jorganchem.2017.06.017
0022-328X/

the form of neutral and ionic structures of chelating bidentate diphosphine ligands. Nevertheless, no study has been carried out of the monodentate bonding of this kind of ligand.

Here we present the synthesis and structure determination, by single crystal X-ray diffraction and spectroscopic techniques, of half sandwich neutral complexes of organometallic Ru(II)-*p*-cymene with two different kinds of P and N-donor ligands of 1,1-bis(diphenyl phosphino)methane (dppm) and *tert*-butylpyridine (tbp), respectively. The complexes have general structures of [Ru(*p*-cymene)(L)Cl_2], where (L) = dppm and tbp and (*p*-cymene) = η^6-*p*-cymene. As a consequence of their particular chemical structure, dichloro ligands are believed to display similar activity to the *cis*-dichloro motif of the well-established anticancer drug cisplatin. We investigated the ability of these two complexes to inhibit the growth of the breast cancer cell lines MCF-7 and HCC1937, and also their anti-bacterial and anti-fungal activities. The [Ru(*p*-cymene)(dppm)Cl_2] complex is more encouraging than pyridine ligand and cisplatin for the treatment of breast cancer.

2. Experimental section

2.1. Materials

The chemicals of [RuCl(η^6-*p*-cymene)(μ-Cl)]$_2$ were purchased from Merck, *tert*-butylpyridine (tbp) was obtained from Sigma-Aldrich. The tetrahydrofuran, diethyl ether and acetonitrile solvents were reagent grades from RCI Labscan and used as received without any further purification.

2.2. Instrumentation

The melting points were determined using a Thomas HOOVER, Unimelt 0–360 °C apparatus. FTIR spectra (KBr disk, 4000–400 cm^{-1}) were recorded with a BX PerkinElmer FTIR spectrophotometer. ^{1}H NMR data were measured using a $CDCl_3$ solvent with a Bruker 300 MHz NMR spectrometer. Tetramethylsilane (TMS) was used as an internal standard. The orange single crystal of [Ru(*p*-cymene)(dppm)Cl_2] was obtained by recrystallization and the diffraction collected with a Bruker APEX-II CCD diffractometer with graphite-monochromated Mo Kα radiation (λ = 0.71,073 Å), 33,925 reflections. The diffraction data were obtained by SMART, SAINT v8.34A and SADABS [15]. The structure was solved by ShelXS [16]. The anisotropic thermal parameters were refined to all non-hydrogen. All hydrogen atoms were placed in calculated, ideal positions and refined using a riding model. The *Olex2* [17], *WinGX*v2014.1 [18] and *Mercury*3.8 [19] programs were used to prepare the materials and molecular graphics for publication. Crystallographic data of [Ru(*p*-cymene)(dppm)Cl_2] has been deposited at Cambridge Crystallographic Data Center via http://www.ccdc.cam.ac.uk/data_request/cif (or from the Cambridge Crystallographic Data Center, 12 Union Road, Cambridge CB21EZ, U.K.; fax: +44 1223 336 033 or email deposit@ccdc.cam.ac.uk) with the CCDC1486230 and can be received upon request. The X-ray data are reported as supplementary crystallographic data.

2.3. Synthesis pathway

The complexes of [Ru(*p*-cymene)(dppm)Cl_2] and [Ru(*p*-cymene)(tbp)Cl_2] were synthesized in the same procedure. The starting material of [RuCl((*p*-cymene))(μ-Cl)]$_2$ dimer (0.1837 g, 0.3 mmol) was dissolved in warm THF (15 mL) and stirred continuously for 1 h. The dppm (0.192 g, 0.5 mmol) or tbp (0.2 mL, 1.2 mmol) ligands were slowly added to the warm (40 °C) Ru(II) dimer solutions. Diethyl ether (5 mL) was added for precipitation. The solution was kept at room temperature for over one week. Orange precipitates of [Ru(*p*-cymene)(dppm)Cl_2] and brownish-orange precipitates of [Ru(*p*-cymene)(tbp)Cl_2]) were obtained. The products were filtered and washed twice with diethyl ether and the synthesized complexes crystallized in a mixture of THF:ethylacetate (2:1 ratio) after a week. The resulting crystals of [Ru(*p*-cymene)(dppm)Cl_2] were separated and dried under vacuum. The obtained complexes are readily soluble in DMSO.

2.3.1. Synthesis of [Ru(p-cymene)(dppm)Cl$_2$]

Yield: 69%. Melting point: 178–180 °C. Anal Calcd for RuC35H36P2Cl2 (690.55): C, 60.87; H, 6.02. Found: C, 60.21; H, 6.22. IR: 2985 (νC-H), 1436 (νC = C), 1094 (νP-Ph), 800 (δC-H para disubstituted benzene), 708 (νP-C) cm^{-1}.1H NMR (300 MHz, $CDCl_3$) 12 signals: δ (ppm): 7.61 (dd, 4H, J_{HH} = 6.3 Hz), 7.21 (t, 2H, J_{HH} = 7.2 Hz), 7.10 (t, 4H, J_{HH} = 6.6 Hz), 5.15 (d, 2H, J_{HH} = 6.0 Hz), 4.90 (d, 2H, J_{HH} = 5.4 Hz), 4.60 (d, 4H, J_{HH} = 7.3 Hz), 3.75 (t, 4H, J_{HH} = 6.5 Hz), 2.47 (m, 4H, J_{HH} = 6.9 Hz), 1.91 (s, 3H), 1.85 (t, 2H, J_{HH} = 6.5 Hz), 1.71 (s, 2H), 0.94 (d, 6H, J_{HH} = 6.9 Hz.

2.3.2. Synthesis of [Ru(p-cymene)(tbp)Cl$_2$]

Yield: 61%. Melting point: 178–180 °C. Anal Calcd for RuC19H26NCl2 (690.55): C, 51.70; H, 6.17; N, 3.17. Found: C, 51.48; H, 6.28; N, 3.13. IR: 3073 (νC-H, aromatic ring), 2958 (νC-H, alkyl), 1617 (νC = C), 835 (δC-H para disubstituted benzene) cm^{-1}.1H NMR (300 MHz, CDCl3) 8 signals: δ (ppm): 8.81 (d, 2H, J_{HH} = 6.3 Hz), 7.23 (d, 2H, J_{HH} = 7.2 Hz), 5.38 (d, 2H, J_{HH} = 6.0 Hz), 5.20 (d, 2H, J_{HH} = 5.4 Hz), 2.93 (m, 4H, J_{HH} = 6.9 Hz), 2.06 (s, 3H), 1.24 (d, 2H, J_{HH} = 6.5 Hz), 1.23 (s, 2H). 13C NMR (300 MHz, CDCl3): 163, 115, 122, 103, 97, 83, 77, 35, 30, 27, 18 ppm. The 13C NMR spectrum was assigned on the basis of the proton-decoupled ^{13}C and the HMQC, DEPT 135, DEPT 90 spectra (Supplementary data).

2.4. Antibacterial assay

All compounds were dissolved in dimethyl sulfoxide and tested against *Staphylococcus aureus* ATCC25923, a clinical isolate of methicillin-resistant *S. aureus* (MRSA) SK1, and *Escherichia coli* ATCC25922 by a microdilution method involving a modification of Clinical and Laboratory Standards Institute (CLSI) M07-A9 [20]. The MICs are the lowest concentration of synthesized compounds with visible growth inhibition. Synthesized compounds of higher concentrations than the MIC, and the MIC were streaked onto a nutrient agar plate and incubated under appropriate conditions. The lowest concentration of compounds showing no growth was recorded as the MBC. Vancomycin and gentamicin were used as standard antibacterial agents for positive inhibitory controls.

2.5. Antifungal assay

The MICs of synthesized compounds were determined by a modification of the microbroth dilution CLSI M27-A3 [21] against yeast (*Cryptococcus neoformans* ATCC90113) and a modification of the microbroth dilution CLSI M38-A2 [22] against a clinical isolate of *Microsporum gypseum* MU-SH4. Microtiter plates were incubated at 35 °C for 48 h for *C. neoformans*. The MFCs of the active compounds were determined by the streaking method on Sabouraud's dextrose agar. Amphotericin B was used as a positive inhibitory control for the yeasts.

2.6. Cell culture

Human breast adenocarcinoma cell lines, including MCF-7 (BRCA1 wild type, estrogen receptor (ER) positive) and HCC1937 (BRCA1 mutant, triple-negative breast cancer (TNBC)) were purchased from the American Type Culture Collections (ATCC,

Rockville, MD). MCF-7 cells were grown in Dulbecco's modified eagle's medium (DMEM) without phenol red, while HCC1937 cells were grown in Roswell Park Memorial Institute 1640 medium (RPMI 1640) without phenol red. Both media were supplemented with 10% fetal bovine serum (FBS) and 1% penicillin-streptomycin. All cell lines were cultured at a constant temperature of 37 °C in a 5% carbon dioxide (CO_2) humidified atmosphere.

2.7. In vitro cytotoxicity assay

The cytotoxic effect of both complexes on MCF-7 and HCC1937 cells was performed by the tetrazolium salt reduction (MTT) assay. Ten thousand cells were plated in each well of 96-well culture plates and grown at 37 °C in 5% CO_2. After 24 h of seeding cells, the medium was removed and cells were treated with different concentrations of the two complexes. [Ru(*p*-cymene)(dppm)Cl_2] was dissolved in 1% DMSO at final concentrations of 0.01, 1, 5, 10, 50 and 100 μM and [Ru(*p*-cymene)(tbp)Cl_2] was dissolved in 1% DMSO at final concentrations of 100, 200, 500, 1000 and 2000 μM. The cells were then incubated at 37 °C in 5% CO_2 for 48 h, after which each well was washed twice with 100 μl of phosphate buffered saline (PBS). Then 100 μl of 0.5 mg/mL of 3-[4,5-dimethylthiazol-2-yl]-2,5 diphenyltetrazolium bromide was added and the plates were further incubated at 37 °C in 5% CO_2 for 4 h. Subsequently, the medium was removed and 200 μl of 100% DMSO was added to dissolve the purple formazan crystal. The absorbance of each well was determined spectrophotometrically at 570 nm. The percentage of cell viability was calculated as follows, % cell viability = (absorbance of the ruthenium complex treated cells)/(absorbance of the vehicle treated cells) x 100. The inhibiting concentration of each ruthenium complex that reduced the number of viable cells to 50% (IC_{50}) was derived by plotting log of the percentage cell viability versus concentration. Results were derived from four independent experiments each performed in at least triplicate.

Data are expressed as the standard error of the mean (±S.E.M.). Statistical analysis comparisons of the significant differences between the mean values was performed using one-way ANOVA. A probability of 0.01 or less was deemed statistically significant. The following notation is used throughout the manuscript: *, $p < 0.01$, relative to the control.

3. Results and discussion

3.1. Synthesis and characterization

Two novel ruthenium(II) complexes [Ru(*p*-cymene)(dppm)Cl_2] and [Ru(*p*-cymene)(tbp)Cl_2] were synthesized by the reaction of [RuCl((*p*-cymene))(μ-Cl)]$_2$ with the P and N donors of 1,1-bis(diphenylphosphino) methane and *tert*-butyl pyridine in tetrahydrofuran, respectively (Scheme 1).

The elemental analysis data of both complexes corresponded to the theoretically calculated values. The differences of C, H and N (in [Ru(tbp)(*p*-cymene)Cl_2] complex) percentages between the calculated and experimental values deviate within 0.04–0.6%. The FTIR spectra displayed some characteristic peaks in the 1600-700 cm^{-1} region (see supplementary data, S1). The [Ru(*p*-cymene)(dppm)Cl_2] complex exhibited the stretching modes of *P*-C(Phenyl) at 520 cm^{-1} and 490 cm^{-1} corresponding to the frequencies reported by Jensen and Nielsen, 1963 [23]. *P*-C(alkyl) stretching frequencies appeared in the range of 700–1100 cm^{-1}. The [Ru(*p*-cymene)(tbp)Cl_2] complex showed the stretching modes of C=C and C=N in the

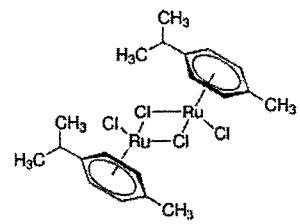

[RuCl(η^6-p-cymene)(μ-Cl)]$_2$

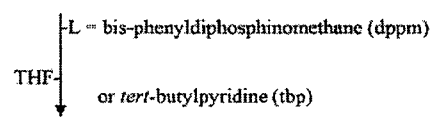

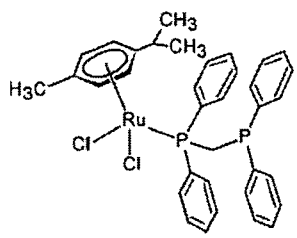

[Ru(dppm)(p-cymene)Cl$_2$]

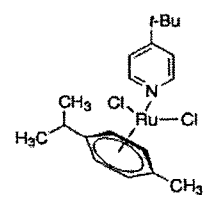

[Ru(tbp)(p-cymene)Cl$_2$]

Scheme 1. Synthesis of the [Ru(dppm)(*p*-cymene)Cl_2] and [Ru(tbp)(*p*-cymene)Cl_2] complexes.

pyridine ring in the region of 1420–1620 cm^{-1}. Importantly, these peaks do not exist in the FTIR spectrum of the starting material, [RuCl(*p*-cymene)(μ-Cl)]$_2$, which is evidence that the functional ligand coordinated with the Ru(II) center. The vibrational frequencies of C=C and C=N were compared with the free 4-*tert*-butylpyridine which are in the range of 1500–1700 cm^{-1}. A shift of *ca.* 100 cm^{-1} was observed. This red shifting frequency may be a result of the decrease of C=C and C=N bond order caused by π-backbonding from the d-orbital of Ru(II) to the π* orbital of the pyridine moiety. Likewise, the C-P stretching mode of [Ru(*p*-cymene)(dppm)Cl_2] is different from its free dppm ligand (1000 cm^{-1} [24]) for almost 500 cm^{-1}.

For ^{1}H NMR spectra (see supplementary data, S2) of both complexes measured in $CDCl_3$, the prospective resonances are detected for the (*p*-cymene) and the functional ligands of dppm and tbp. In consequence of the coordination of the functional ligands, downfield shifts of 0.15–0.25 ppm of the ligand ring protons are noticed in comparison with the free ligands. Likewise, downfield shifts were also found for the coordinated (*p*-cymene) in both complexes compared to the *p*-cymene ligand in RuCl(*p*-cymene)(μ-Cl)]$_2$ complex. The chemical shifts are presented in the experimental section. The ^{13}C NMR spectra (see supplementary data, S3) of [Ru(*p*-cymene)(tbp)Cl_2] are in good agreement with the resonance signals of its structure.

The structure of the [Ru(*p*-cymene)(dppm)Cl_2] complex was determined by single crystal x-ray diffraction. Its molecular structure with atom numbering is displayed in Fig. 1, selected bond lengths and angles are given in Table 1. The crystal structure of [Ru(*p*-cymene)(dppm)Cl_2] is a triclinic system with a *P*-1 space group. The mononuclear complex of Ru(II) is in four coordinations with π conjugated carbons in cymene, and in dppm through one of the phosphorus atoms and two choro ligands show the piano-stool distorted psuedo-tetrahedral geometry. The Ru-C(*p*-cymene) lengths are between 2.161(4)and 2.235(3) Å; the average distance between Ru(II) and the centroid of the *p*-cymene ring is 1.6941(16) Å; and the average length of Ru-Cl is 2.4095(9) Å. All these measurements are similar to the relevant complexes in Refs. [25,26]. The length of Ru-P is 2.350(8) Å which is also close to the other compounds [27,28]. The bond angles around Ru(II) are in the range of 82.45(3)° to 160.65(10)°. The largest angle can be observed in the C(2)-Ru-P(1). It is probably due to the steric bulk of the phosphinomethane groups. In the molecular structure, intramolecular π-π stacking is observed of the two opposed phenyl rings in the dppm ligand. The centroid-centroid distance is 3.955(3) Å as shown in Fig. 2. In addition, there is intermolecular π-π stacking of two dppm phenyl rings and π-π stacking between the cymene and dppm phenyl rings of two alternate adjacent molecules (Fig. 2). This stabilizes the crystal packing with a centroid-centroid (Cg5—Cg5) distance of 4.328(3) Å. The π-π stacking between the cymene ring (Cg1) and the phenyl ring (Cg2) of dppm, Cg1—Cg2 stabilizes at 4.460(2) Å.

In addition, the intermolecular contacts in the packing were

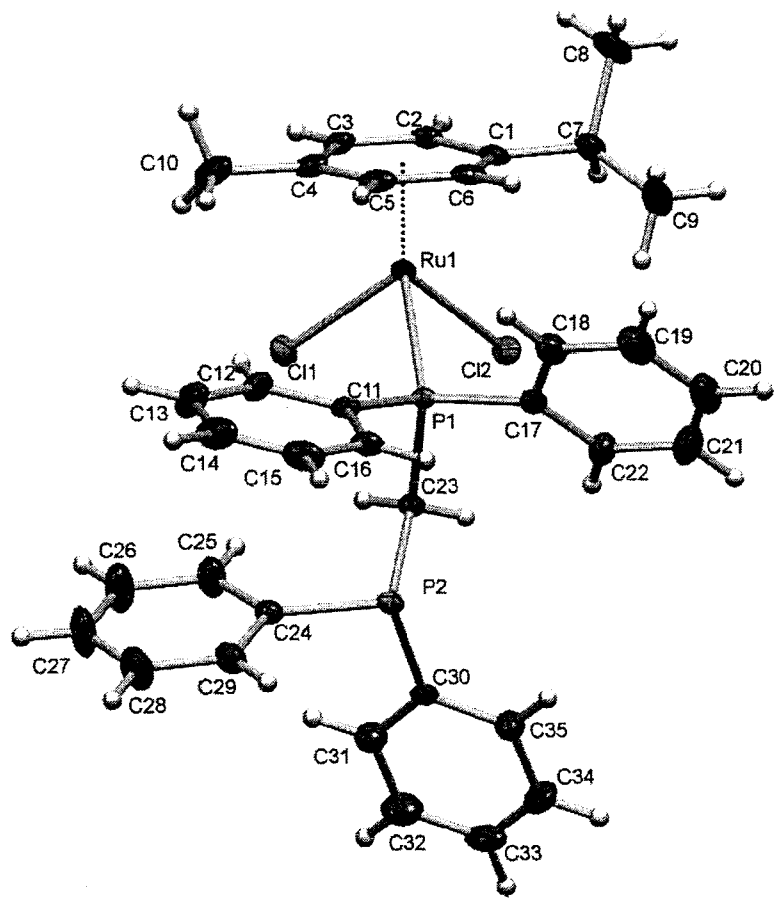

Fig. 1. An ORTEP structure of [Ru(*p*-cymene)(dppm)Cl_2] complex with atom numbering.

Table 1
Selected bond lengths (Å) and bond angles (°) of [Ru(*p*-cymene)(dppm)Cl_2] complex.

Ru(1)-P(1)	2.3500(8)
Ru(1)-ring centroid	1.6941(16)
Ru(1)-Cl(1)	2.4150(9)
Ru(1)-Cl(2)	2.4040(9)
P(1)-C(11)	1.825(3)
P(1)-C(17)	1.823(4)
P(1)-Ru(1)-Cl(1)	87.85(3)
P(1)-Ru(1)-Cl(2)	88.78(3)

studied by Hirshfeld surface analysis. The Crystal Explorer program (Wolff et al., 2012) [28] was used to generate Hirshfeld surfaces mapped over d_{norm}. The mapping of d_{norm} was used to analyze the intermolecular contact distances, d_i and d_e, from the Hirshfeld surfaces between the nearest atom inside and outside molecules, respectively. Hirshfeld surfaces mapped over d_{norm}, shown in Fig. 3, reveal a pair of hydrogen-bonds representing acceptors on the surfaces and they are shown as bright-red spots at Cl1 of C2-H2···Cl1(#1) and at Cl2 of C3-H3···Cl2(#1) with distances of 3.725(4) and 3.529(4) Å, respectively (for symmetry operation #1: x, 1-y, 1-z). Two-dimensional fingerprint plots (Rohl et al., 2008) [29] are shown in Fig. 4 as the combination of d_e and d_i and provide a summary of intermolecular contacts in the crystal. The overall two-dimensional fingerprint plot is depicted in Fig. 4a, and those for the contacts of H—H, H—Cl/Cl···H, C—H/H···C are shown in Fig. 4b–d. The greatest contribution to the overall Hirshfeld surface, i.e. 72.8%, is provided by H—H contacts in crystal packing. The contribution of 9.9% from the H—Cl/Cl···H contacts corresponds to the C—H···Cl interactions, which are represented by a pair of asymmetric spikes at $d_e + d_i$ *ca* 3.2 A° (Fig. 4c). The asymmetrical peaks of the delineated finger print plot of Fig. 4d, indicate C—H/H···C contacts with 14.3%, $d_e + d_i$ *ca* 3.6 Å, representing π-π stacking interactions in crystal packing.

3.2. Absorption

The absorption spectra of the [Ru(*p*-cymene)(dppm)Cl_2] and [Ru(*p*-cymene)(tbp)Cl_2] complexes (Fig. 5) in chloroform were measured in the range of 200–800 nm. The absorption bands of [Ru(*p*-cymene)(dppm)Cl_2] and [Ru(*p*-cymene)(tbp)Cl_2] complexes in the visible region appear at the maximum wavelengths of absorption at 397 nm and 420 nm, respectively, providing low molar extinction coefficients (<1700 $M^{-1}cm^{-1}$) which are ascribed to DMSO-d_6 transition of Ru(II). In contrast, π-π^* transition with high molar extinction coefficients (>10,000 $M^{-1}cm^{-1}$) is to be found in the non-visible UV region.

3.3. Antimicrobial activity of the [Ru(*p*-cymene)(dppm)Cl_2] and [Ru(*p*-cymene)(tbp)Cl_2] complexes

Using the agar microdilution method, we tested the antimicrobial activity of the two studied compounds against three types of bacteria, namely *S. aureus* (SA), methicillin - resistant *S. aureus* (MRSA) and *E. coli* ATCC25922 (EC). Growth inhibition was compared with that of the antibacterial drugs, vancomycin and gentamicin. In addition, we measured the antifungal activity of the complexes against one type of yeast (*C. neoformans* ATCC 90,113). A comparison of these results with those produced by the standard antifungal drug amphotericin B is presented in Table 2. No activity was found from checking against each tested organism.

The [Ru(*p*-cymene)(dppm)Cl_2] complex shows antibacterial activities at concentrations < 32 $\mu g\ mL^{-1}$. However, the [Ru(*p*-cymene)(tbp)Cl_2] complex does not exhibit such activities in the studied system. The results imply that the dppm ligand may have a strong influence on the bacterial growth inhibition mechanism not shown by the free ligand. The [Ru(*p*-cymene)(dppm)Cl_2] complex significantly inhibited *Staphylococcus aureus ATCC25923, MRSA = methicillin - resistant Staphylococcus aureus* with MIC/MBC values of 8/200 and 32/128 $\mu g\ mL^{-1}$, respectively. The variation in the antimicrobial activity of the free ligand and the different metal complexes against the different microorganisms is due either to the differences in the ribosomes in the microbial cells or the impermeability of the microbe cells. It is worth noting that chelation is able to increase the ability of the complexes to permeate the microorganism cell membranes by decreasing the polarizability of the metal, as explained by Tweedy's chelation theory [30]. The

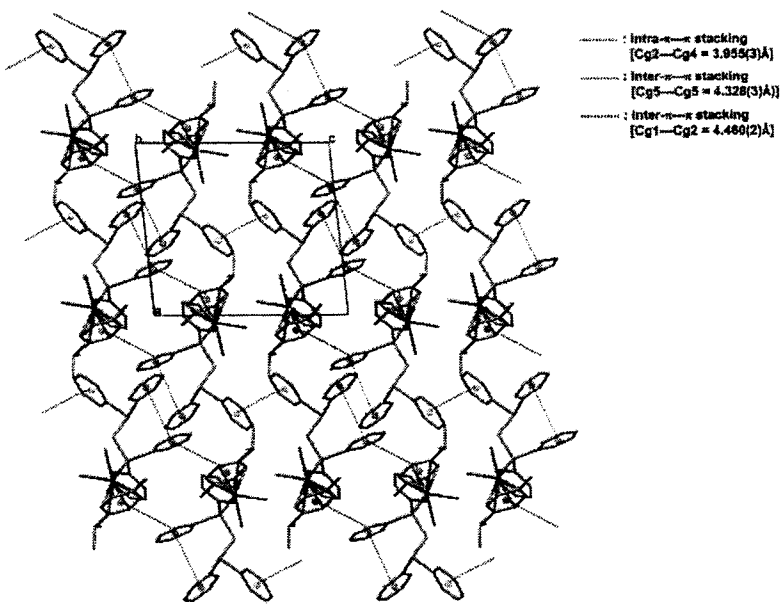

Fig. 2. The packing interactions of [Ru(*p*-cymene)(dppm)Cl_2] complex.

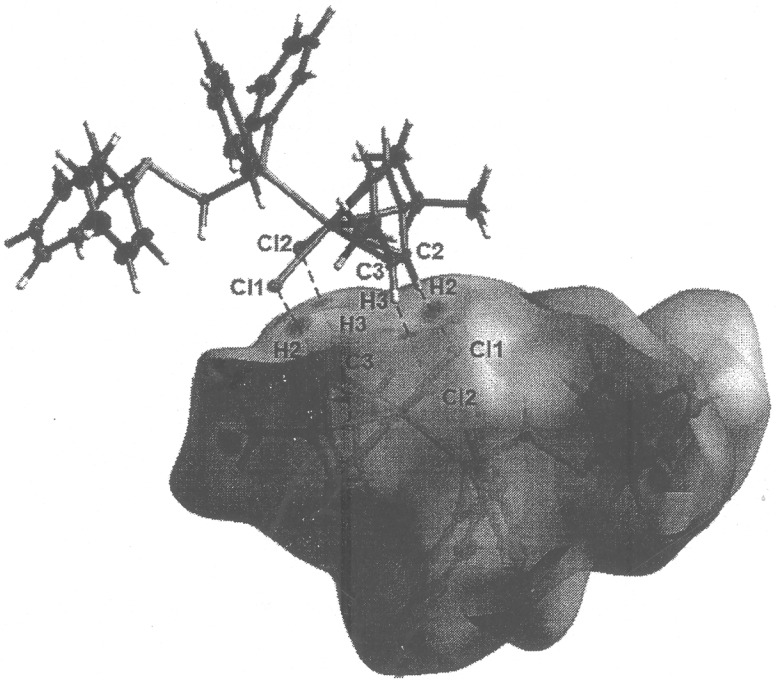

Fig. 3. Hirshfeld surface analysis mapped for [Ru(*p*-cymene)(dppm)Cl_2] complex over d norms showing hydrogen bonds of C-H—Cl with neighboring molecules.

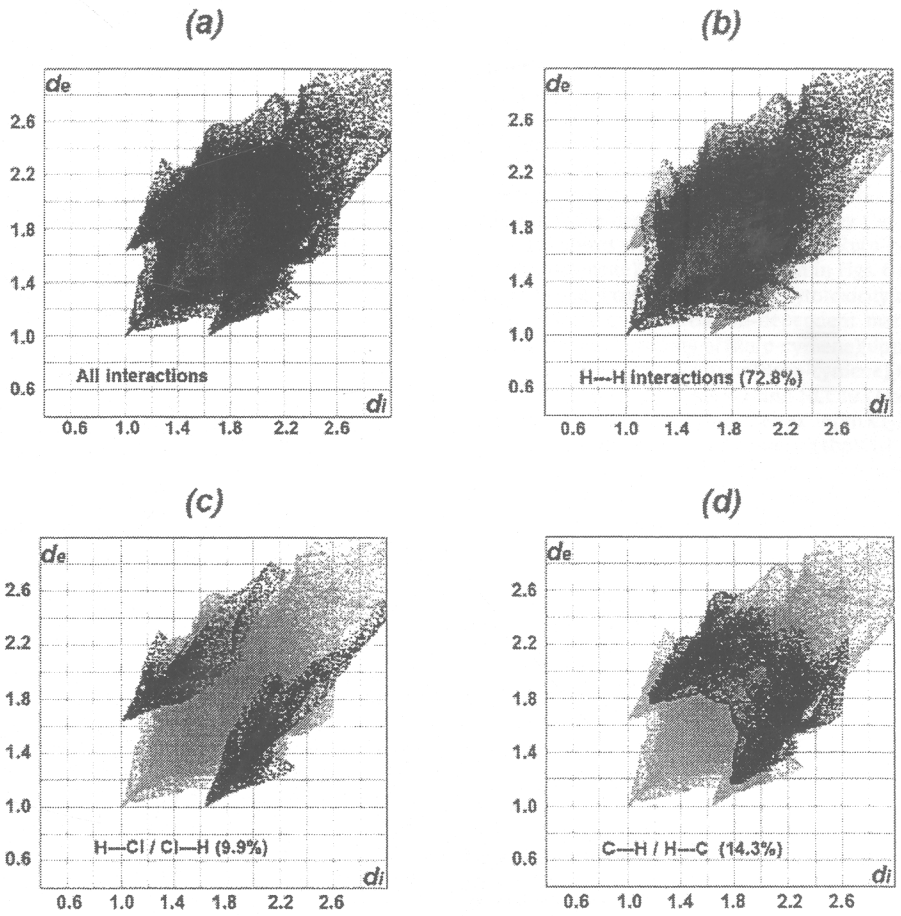

Fig. 4. Two-dimensional fingerprint plots of [Ru(*p*-cymene)(dppm)Cl_2] complex: (a) overall interactions and pictured into contributions from different contacts, (b) H—H,(c) H—Cl/Cl—H and (d) C—H/H—C, respectively.

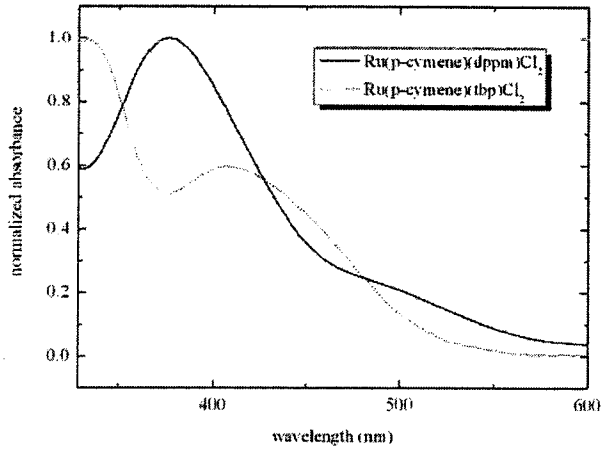

Fig. 5. Normalized absorption spectra of [Ru(*p*-cymene)(dppm)Cl_2] and [Ru(*p*-cymene)(tbp)Cl_2].

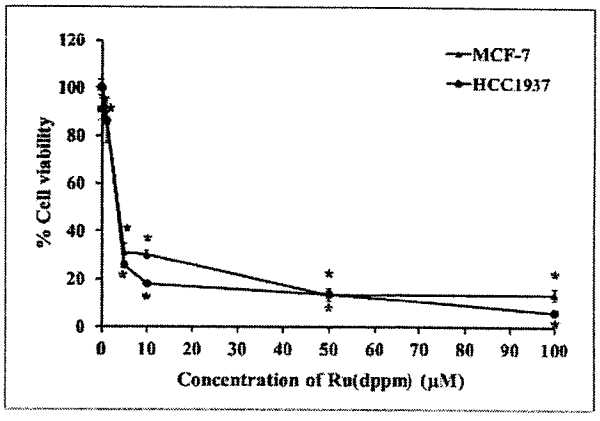

Fig. 6. Antiproliferative effect of [Ru(*p*-cymene)(dppm)Cl_2] on human breast cancer cells using the MTT assay. MCF-7 and HCC1937 cells were treated with various concentrations of [Ru(*p*-cymene)(dppm)Cl_2] at 37 °C in 5% CO_2 for 48 h. Each result point was the percentage of cell viability mean values ± standard error obtained from four independent experiments.

Table 2
Antimicrobial activity levels of [Ru(*p*-cymene)(dppm)Cl_2] and [Ru(*p*-cymene)(tbp)Cl_2] complexes and starting materials in dmso.

Compounds	Bacteria (μg/mL)						Yeast (μg/mL)	
	SA		MRSA		EC		CN90113	
	MIC	MBC	MIC	MBC	MIC	MBC	MIC	MFC
[Ru(dppm)(pcymene)Cl_2]	8	200	32	128	NA	NA	64	128
[Ru(tbp)(*p*-cymene)Cl_2]	NA	NA	NA	NA	NA	NA	NA	NA
[[RuCl((*p*-cymene)(μ-Cl)]$_2$]	NA	NA	NA	NA	NA	NA	NA	NA
dppm	NA	NA	NA	NA	NA	NA	NA	NA
tbp	0.5	NA	NA	NA	NA	NA	NA	NA
Vancomycin	–	1	1	2	–	–	–	–
Gentamicin	–	1	1	–	0.5	–	–	–
Amphotericin B		–	–	–	–	–	0.25	0.5

SA = *Staphylococcus aureus* ATCC25923, MRSA = methicillin - resistant *Staphylococcus aureus*, *Escherichia coli* ATCC25922, CN90113 = *Cryptococcus neoformans* ATCC90113 flucytosine - resistant MIC = minimum inhibitory concentration (μg/mL), MBC = minimum bactericidal concentration (μg/mL), MFC = minimum fungicidal concentration (μg/mL), NA = non active.

[Ru(*p*-cymene)(dppm)Cl_2] has a more lipophilic structure than that of the [Ru(*p*-cymene)(tbp)Cl_2] due to the extra phenyl rings in the diphosphinomethane group. Penetration through the cell walls of bacteria is, therefore, much more possible than it is with the [Ru(*p*-cymene)(tbp)Cl_2] complex, leading to greater inhibition of bacterial growth.

The data obtained from the experiments suggested that the [Ru(*p*-cymene)(dppm)Cl_2] compound exhibits mild to good antifungal activity. Interestingly, the compound was more effective against bacteria than against fungi.

3.4. Anticancer activity

The antiproliferative property of the new ruthenium(II)arene complexes, [Ru(*p*-cymene)(dppm)Cl_2] and [Ru(*p*-cymene)(tbp)Cl_2] were tested in two different human breast cancer cells using the MTT assay. The percentage of cell viability was assessed as shown in Figs. 4 and 5. As can be seen in Fig. 6, for each type of breast cancer cell, the observed cell growth inhibitory effect of [Ru(*p*-cymene)(dppm)Cl_2] varied at similar concentrations. The same results for the [Ru(*p*-cymene)(tbp)Cl_2] complex show clear differences at concentrations from 100 μM to 1000 μM, and no variation at concentrations from 1000 μM to 2000 μM. Representative results showed that the percentage cell viability of both breast cancer cells decreased as concentrations of [Ru(*p*-cymene)(dppm)Cl_2] and [Ru(*p*-cymene)(tbp)Cl_2] increased. The cytotoxic activities of the ruthenium complexes, compared to cisplatin, were determined as the IC_{50} values and are summarized in Table 3. Both ruthenium complexes can inhibit breast cancer cell growth, but with different cellular responses. Interestingly, [Ru(*p*-cymene)(dppm)Cl_2] exhibited significantly greater cytotoxicity than [Ru(*p*-cymene)(tbp)Cl_2] against cells of both cisplatin-resistant MCF-7 and cisplatin-sensitive, BRCA1-defective HCC1937.

A feature of the antiproliferative activity studies was tested as chemotherapeutic agents candidates for both cisplatin-resistant, BRCA1-competent MCF-7 and cisplatin-sensitive, BRCA1-deficient, triple-negative HCC1937 cells by the two ruthenium(II) arene complexes with different ligands, [Ru(*p*-cymene)(dppm)Cl_2] and [Ru(*p*-cymene)(tbp)Cl_2] as shown in Figs. 6 and 7 and Table 3. Both ruthenium complexes exerted cytotoxicity against both breast cancer cells in a concentration-dependent manner. It was of interest that the cytotoxicity of [Ru(*p*-cymene)(dppm)Cl_2] was clearly greater than that of cisplatin or [Ru(*p*-cymene)(tbp)Cl_2] against all breast cancer cells. Both MCF-7 and HCC1937 cells were 16 times more sensitive to the [Ru(*p*-cymene)(dppm)Cl_2] than to cisplatin. Compared to cisplatin, [Ru(*p*-cymene)(tbp)Cl_2] was less cytotoxic to the same cells by factors of 15 and 16 respectively. Compared to [Ru(*p*-cymene)(dppm)Cl_2], it was respectively 247 and 275 times less cytotoxic. The greater cytotoxicity of [Ru(*p*-cymene)(dppm)Cl_2]

Table 3
IC_{50} mean values (μM) for [Ru(*p*-cymene)(dppm)Cl_2], [Ru(*p*-cymene)(tbp)Cl_2], and cisplatin against MCF-7 and HCC1937 cells after 48 h of treatment. (All data are the mean and standard errors obtained from four independent experiments, each performed in at least triplicate).

Metal complexes	IC_{50} (μM)	
	MCF-7	HCC1937
Cisplatin [36]	$42.2 \pm 8^{*,**}$	$23.4 \pm 7^{*,**}$
[Ru(*p*-cymene)(dppm)Cl_2]	$2.6 \pm 0.2^{*,**}$	$1.4 \pm 0.3^{*,**}$
[Ru(*p*-cymene)(tbp)Cl_2]	$642.6 \pm 6.6^{*,**}$	$385.1 \pm 5.3^{*,**}$

Statistical significance differences are indicated by $^{*}p < 0.01$, compared to the IC_{50} values of the same complex on cell lines, and $^{**}p < 0.001$, compared to the IC_{50} values of the complexes on each cell line.

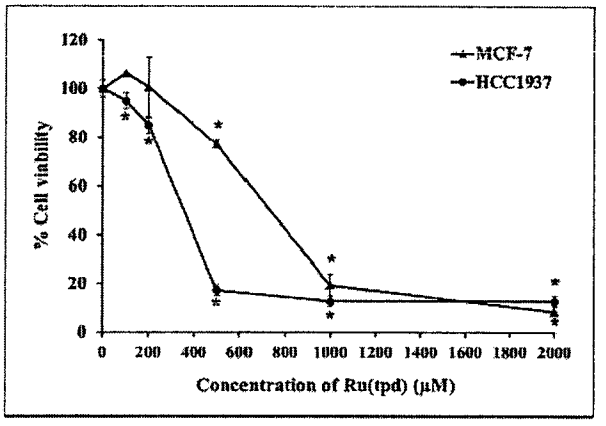

Fig. 7. Antiproliferative effect of [Ru(*p*-cymene)(tbp)Cl_2] on human breast cancer cells using the MTT assay. MCF-7 and HCC1937 cells were treated with various concentrations of [Ru(*p*-cymene)(tbp)Cl_2] at 37 °C in 5% CO_2 for 48 h. Each result point was the percentage of cell viability mean values ± standard error obtained from four independent experiments.

may be attributed to the larger size and surface area of its structure and the effect that has on the activity of the coordinated diphenylphosphino ligand. The hydrophobicity of the complex, and its π-extended system could also be associated with its superior uptake into breast cancer cells [31]. These results agree very well with a previous study which showed that ruthenium(II) complexes containing 1,1′-bis(diphenylphosphino) ferrocene (dppf) exerted an enhanced anticancer activity against S-180 murine ascetic sarcoma 180, DU145 human prostate carcinoma, K562 chronic myeloid leukemia and A549 human lung carcinoma [32]. It was also interesting that HCC1937, known to be a BRCA1-defective (5382insC mutation) cell line lacking an estrogen receptor (ER), was significantly more sensitive than the BRCA1-competent MCF-7 cell line. Ruthenium sensitivity in the BRCA1-mutated cells might be related to dysfunctional BRCA1 that is unable to repair DNA damage induced by [Ru(*p*-cymene)(dppm)Cl_2] treatment, ultimately leading to breast cancer cell death [33–36]. However, the precise molecular mechanisms of action of this ruthenium(II)-arene complex remain largely unexplored and are of great interest for further investigation. Our results are the first evidence of the anticancer activity of [Ru(*p*-cymene)(dppm)Cl_2] against both cisplatin-resistant and BRCA1-defective breast cancer cells. Therefore, the ruthenium(II) arene complex containing diphenylphosphino ligand could be a promising therapeutic ruthenium-based agent for breast cancers.

4. Conclusion

The structures of half sandwich [Ru(*p*-cymene)(dppm)Cl_2] and [Ru(*p*-cymene)(dppm)Cl_2] complexes are pseudo-tetrahedral distorted geometry. The [Ru(*p*-cymene)(dppm)Cl_2] complex presents as a promising powerful anticancer against MCF-7 and HCC1937 breast cell lines with a lower IC_{50} than that of cisplatin, while [Ru(*p*-cymene)(tbp)Cl_2] shows much lower activity. It is favored by the diphosphine ligand more than the pyridine moiety. Although the mechanism of the inhibition of growth in cancer cells is not yet well understood, the binding of synthesized ruthenium complexes to DNA cancer cells is the main reason for their anticancer effect. Chloro ligands are labile which can cause further hydrolysis and allow Ru(II) to attach to base pairs of DNA cancer cells. The [Ru(*p*-cymene)(dppm)Cl_2] exhibits moderate to good activity against SA and MRSA bacteria but only weak inhibition of CN yeast growth.

Acknowledgement

NL acknowledges financial support from the Prince of Songkla University under contract number (SCI560355S) as well as Center for Innovation in Chemistry (PERCH–CIC), the Commission on Higher Education and the Ministry of Education and Faculty of Science, PSU. AR thanks the National Research Council of Thailand and Prince of Songkla University (PHA570058S, PHA580500S, PHA580926S and PHA590396S) for financial support. We are grateful to the Pharmaceutical Laboratory Service Center, Faculty of Pharmacuetical Sciences, Prince of Songkla University for research facilities. We would also like to thank Mr.Thomas Duncan Coyne for assistance with the English.

Appendix A. Supplementary data

Supplementary data related to this article can be found at http://dx.doi.org/10.1016/j.jorganchem.2017.06.017.

References

[1] A. Kumar, A. Kumar, R.K. Gupta, R.P. Paitandi, K.B. Singh, S.K. Trigun, M.S. Hundal, D.S. Pandey, J. Organomet. Chem. 801 (2016) 68–79.
[2] J.Q. Wang, P.Y. Zhang, L.N. Ji, H. Chao, J. Inorg. Chem. 146 (2015) 89–96.
[3] S. Thangavel, M. Paulpandi, H.B. Friedrich, K. Murugan, S. Kalva, A.A. Skelton, J. Inorg. Biochem. 159 (2016) 50–61.
[4] C.S. Allarodyce, J.D. Paul, J.E. David, A.S. Paul, S. Rosario, J. Organomet. Chem. 668 (2003) 35–42.
[5] G.-S. Sanja, I. Ivanka, R. Gordana, T. Nina, G.L. Nevenka, R. Sinisa, B.A. Vladimir, K.K. Bernhard, L.J.T. Živoslav, Med. Chem. 45 (2010) 1051–1058.
[6] K. Wolfgang, G.H. Christian, A.N. Alexey, L.K. Maxim, O.J. Roland, B. Caroline, A.J. Michael, B.A. Vladimir, K.K. Bernhard, Organomet 28 (2009) 4249–4251.
[7] F. Beckford, D. Dourth, M. Shaloski Jr., J. Didon, J. Thessing, J. Woods, V. Crowell, N. Gerasimchuk, A. Gonzalez-Sarrias, N.P. Seeram, J. Inorg. Biochem. 105 (2011) 1019–1029.
[8] A.V. Carsten, K.R. Anna, S. Rosario, J. Lucienne, J.D. Paul, Eur. J. Inorg. Chem. (2008) 1661–1671.
[9] L. Bíró, D. Hűse, A.C.S. Benyei, P. Buglyo, J. Inorg. Biochem. 116 (2012) 116–125.
[10] A.K. Renfrew, A.E. Egger, R. Scopelliti, C.G. Hartinger, P.J. Dyson, Comptes Rendus Chim. 13 (2010) 1144–1150.
[11] C. Scolaro, C.G. Hartinger, C.S. Allardyce, B.K. Keppler, P.J. Dyson, J. Inorg. Biochem. 102 (2008) 1743–1748.
[12] X. Shang, T.F.S. Silva, L.M.D.R.S. Martins, Q. Li, M.F.C. Guedes da Silva, M.L. Kuznetsov, A.J.L. Pombeiro, J. Organomet. Chem. 730 (2013) 137–143.
[13] G. Gasser, I. Ott, N.M. Nolte, J. Med. Chem. 54 (2011) 3–25.
[14] A.R. Bárzano, R.M. Lord, A.M. Basri, R.M. Phillips, A.J. Blacker, P.C. McGowan, Dalton Trans. 44 (2015) 3265–3270.
[15] Bruker, SMART, SAINT and SADABS, Bruker AXS Inc, Madison,Wisconsin, USA, 2013.
[16] O.V. Dolomanov, L.J. Bourhis, R.J. Gildea, J.A.K. Howard, H. Puschmann, J. Appl. Cryst. 42 (2009) 339–341.
[17] G.M. Sheldrick, Acta Cryst. A71 (2015) 3–8.
[18] L.J. Farrugia, J. Appl. Cryst. 45 (2012) 849–854.
[19] C.F. Macrae, I.J. Bruno, J.A. Chisholm, P.R. Edgington, P. McCabe, E.R.M. Pidcock, L. Rodriguez-Monge, R. Taylor, J. van de Streek, P.A. Wood, J. Appl. Cryst. 41 (2008) 466–470.
[20] Clinical and Laboratory Standards Institute (CLSI), Methods for Dilution Antimicrobial Susceptibility Tests for Bacteria that Grow Aerobically; Approved Standard, nineth ed., CLSI, Wayne, 2012. CLSI document M07–A9.
[21] Clinical and Laboratory Standards Institute (CLSI), Reference Method for Broth Dilution Antifungal Susceptibility Testing of Yeasts; Approved Standard, third ed., CLSI, Wayne, 2008a. CLSI documents M27–A3.
[22] Clinical and Laboratory Standards Institute (CLSI), Reference Method for Broth Dilution Antifungal Susceptibility Testing of Filamentous Fungi; Approved Standard, second ed., CLSI, Wayne, 2008b. CLSI documents M38–A2.
[23] K.A. Jensen, P.H. Nielsen, Acta Chim. Scand. 17 (1963) 1875–1885.
[24] H.G. Horn, K. Sommer, Spectrochim. Acta 27A (1971) 1049–1054.
[25] D. Schleicher, A. Tronnier, H. Leopold, H. Borrmann, T. Strassner, Dalton Trans. 45 (2016) 3260–3263.
[26] H. Rosana, K. Jakob, K. Wolfgang, R. Urska, T. Boris, G.H. Christian, K.K. Bernhard, M. Damijan, T. Iztok, Organomet 31 (2012) 5867–5874.
[27] A.V. Carsten, K.R. Anna, S. Rosario, J. Lucienne, J.D. Paul, Eur. J. Inorg. Chem. (2008) 1661–1671.
[28] S.K. Wolff, D.J. Grimwood, J.J. Mckinnon, M.J. Turner, D. Jayatilaka, M.A. Spackman, Crystal Explorer, The University of Western Australia, 2012.

[29] A.L. Rohl, M. Moret, W. Kaminsky, K. Claborn, J.J. Mckinnon, B. Kahr, Cryst. Growth &Des 8 (2008) 4517–4525.
[30] M. Muthukumar, P. Viswanathamurthi, Spectrochim. Acta Part A 74 (2009) 454–462.
[31] S. Das, S.R. Sinha, K. Britto, A.G. Somasundaram Samuelson, J. Inorg. Biochem. 104 (2010) 93–104.
[32] F.C. Pereira, B.A. Lima, A.P. de Lima, W.C. Pires, T. Monteiro, L.F. Magalhães, W. Costa, A.E. Graminha, A.A. Batista, J. Ellena, E.P. Siveira-Lacerda, J. Inorg. Biochem. 149 (2015) 91–101.
[33] E. Alli, V.B. Sharma, A.R. Hartman, P.S. Lin, L. McPherson, J.M. Ford, BMC Pharmacol. (2011) 11–17.
[34] R.M. Neve, K. Chin, J. Fridlyand, J. Yeh, F.L. Baehner, T. Fevr, L. Clark, N. Bayani, J.P. Coppe, F. Tong, T. Speed, P.T. Spellman, S. DeVries, A. Lapuk, N.J. Wang, W. LinKuo, J.L. Stilwell, D. Pinkel, D.G. Albertson, F.M. Waldman, F. McCormick, R.B. Dickson, M.D. Johnson, M. Lippman, S. Ethier, A. Gazdar, J.W. Gray, Cancer Cell. 10 (2006) 515–527.
[35] P. Tassone, M.T. Di Martino, M. Ventura, A. Pietragalla, I. Cucinotto, T. Calimeri, A. Bulotta, P. Neri, M. Caraglia, P. Tagliaferri, Cancer Biol. Ther. 8 (2009) 648–653.
[36] T. Nhukeaw, P. Temboot, K. Hansongnern, A. Ratanaphan, BMC Cancer 14 (2014) 73.

Supplymentary data

ผลการทดสอบ cytotoxicity ต่อ vero cell ของสารประกอบเชิงซ้อน

[Ru(p-cymene)(dppm)Cl_2]

Test: Cytotoxicity against Vero cells (African green monkey kidney)
Method: Green Fluorescent Protein (GFP)-based assay
IC_{50} of positive control: Ellipticine = 1.43 µg/ml
Reported date (dd/mm/yy): 17/08/2016
Total number of sample: 2

Item	Screening code	Sample code	Final concentration (µg/ml)	Fluorescence unit at Day0		Fluorescence unit at Day4		% Cytotoxicity	Activity	IC_{50} (µg/ml)
				Average	SD	Average	SD			
	Negative	Cell+DMSO	0.5% DMSO	1621	67	2768	182	0.00	-	-
	Positive	Ellipticine	4.00	1659	61	1737	124	93.15	Cytotoxic	
			2.00	1610	72	1896	136	75.03	Cytotoxic	1.43
			1.00	1635	39	2510	140	23.65	Non-cytotoxic	
			0.50	1672	49	2638	138	15.77	Non-cytotoxic	
			0.25	1668	50	2755	175	5.13	Non-cytotoxic	
			0.13	1654	52	2759	197	3.59	Non-cytotoxic	
1	VA0549*	Ru (dppm)	50.00	1464	80	1474	113	99.11	Cytotoxic	19.94
			16.67	1565	49	2318	124	34.37	Non-cytotoxic	
			5.56	1574	43	2885	100	-14.34	Non-cytotoxic	
			1.85	1555	96	2907	82	-17.92	Non-cytotoxic	
			0.62	1637	40	2978	57	-16.96	Non-cytotoxic	
			0.21	1614	36	2989	125	-19.88	Non-cytotoxic	
2	VA0550*	dppm	50.00	1534	100	2824	109	-12.56	Non-cytotoxic	-
			16.67	1615	62	3008	98	-21.48	Non-cytotoxic	-
			5.56	1632	64	3298	89	-45.33	Non-cytotoxic	-
			1.85	1670	18	3005	88	-16.50	Non-cytotoxic	-
			0.62	1689	52	3012	36	-15.46	Non-cytotoxic	-
			0.21	1695	50	3041	43	-17.40	Non-cytotoxic	-

Remark: *Partially soluble in 100% DMSO

Assayed by Kitlada S. (Kitlada Srichomthong) (17 / 08 / 16)

Approved by Kannawat D. (Kannawat Danwisetkanjana) (17 / 08 / 16)

Interpretation

% Cytotoxicity	Activity
< 50%	Non-cytotoxic
≥ 50%	Cytotoxic (IC_{50} included)

National Center for Genetic Engineering and Biotechnology (BIOTEC), National Science and Technology Development Agency (NSTDA)
113 Phaholyothin Road, Khlong Nueng, Khlong Luang, Pathum Thani 12120, Thailand
Tel. 02-5646629, Fax 02-5646707, Email: bioassayservice@biotec.or.th, www.biotec.or.th/bioassay

ผลการทดสอบการยับยั้งเซลล์มะเร็งเต้านม MCF-7 ของสารประกอบเชิงซ้อน

[Ru(p-cymene)(dmazpy)Cl]Cl และ [Ru(p-cymene)(deazpy)Cl]Cl

Test: Anti-Cancer (MCF7-breast cancer)
Method: Resazurin Microplate assay (REMA)
IC_{50} of positive control: Tamoxifen = 8.72 µg/ml, Doxorubicin = 8.89 µg/ml
Reported date (dd/mm/yy): 27/03/2014
Total No. of tested sample: 5

Item	Screening code	Sample code	Final concentration (µg/ml)	Fluorescence unit		% Inhibition	Activity	IC_{50} (µg/ml)
				Average	SD			
	Negative	Cell+DMSO	0.5% DMSO	7940	327	-	-	-
	Positive1	Tamoxifen	40.00	723	51	99.69	Active	
			20.00	786	51	98.83	Active	
			10.00	3607	203	59.85	Active	8.72
			5.00	6330	198	22.24	Inactive	-
			2.50	7053	353	12.26	Inactive	-
			1.25	7063	381	12.12	Inactive	-
	Positive2	Doxorubicin	40.00	1097	106	94.53	Active	
			20.00	2246	206	78.65	Active	
			10.00	3564	213	60.45	Active	8.89
			5.00	6662	252	17.65	Inactive	-
			2.50	7239	308	9.68	Inactive	-
			1.25	7204	248	10.17	Inactive	-
1	V9112	ru-dm-pcy	50.00	823	31	98.31	Active	-
2	V9113	ru-de-pcy	50.00	744	38	99.40	Active	-
3	V9114	2de	50.00	7816	510	1.71	Inactive	-
4	V9115	dim-lr	50.00	6874	423	14.72	Inactive	-
5	V9116	lrde	50.00	842	21	98.05	Active	-

Remark:

Assayed by _____
(Pattiyaa Laksanacharoen)
(_ _ / _ _ / _ _)

Approved by _____
(Somjit Komwijit)
(_ _ / _ _ / _ _)

Interpretation

% Inhibition	Activity
< 50%	Inactive
≥ 50%	Active (IC_{50} included)

National Center for Genetic Engineering and Biotechnology (BIOTEC), National Science and Technology Development Agency (NSTDA)
113 Paholyothin Rd, Klong Nueng, Klong Luang, Pathumthani 12120, Thailand
Tel. 02-5646629, Fax 02-5646707, www.biotec.or.th/bioassay

ผลการทดสอบ cytotoxicity ต่อ vero cell ของสารประกอบเชิงซ้อน

[Ru(p-cymene)(dppm)Cl_2]

Supplementary data

Characterization of [Ru(*p*-cymene)(dppm)Cl_2] complex

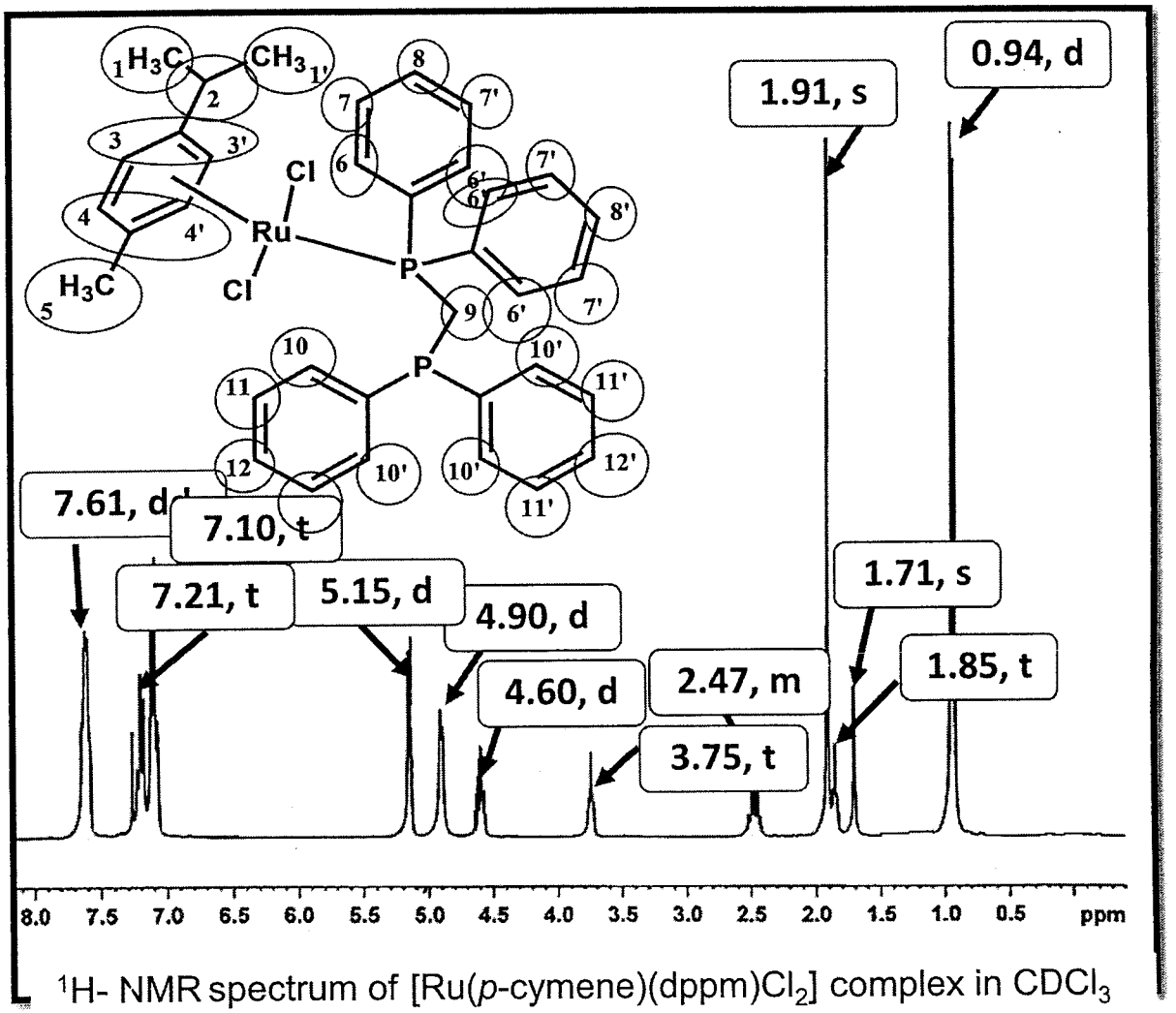

^{1}H- NMR spectrum of [Ru(*p*-cymene)(dppm)Cl_2] complex in $CDCl_3$

Investigate	% Element (SD)		
	%N	% C	% H

Calcd.	-	60.87	6.02
Found	-	60.21(2.17×10^{-2})	6.22(3.09×10^{-2})

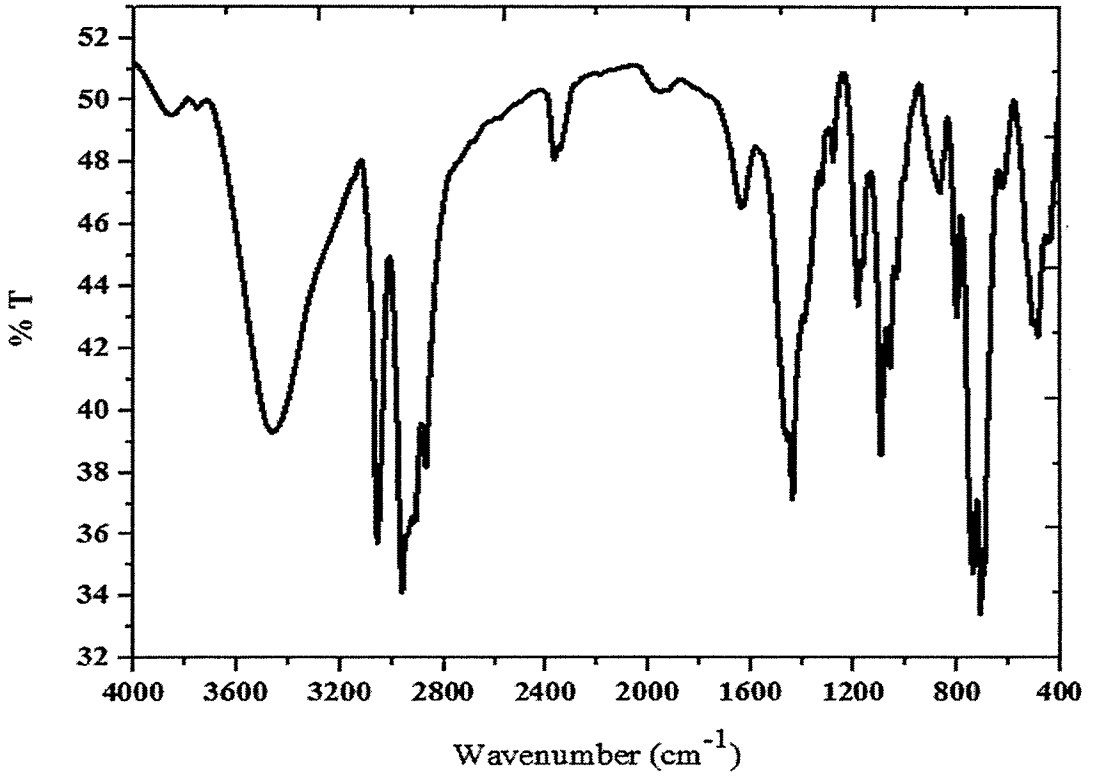

IR spectrum of [Ru(*p*-cymene)(dppm)Cl_2], Ru(dppm) complex.

Table 1. Crystal data and structure refinement for rudppm.

Identification code	shelx	
Empirical formula	C35 H36 Cl2 P2 Ru	
Formula weight	690.55	
Temperature	293(2) K	
Wavelength	0.71073 Å	
Crystal system	Triclinic	
Space group	P -1	
Unit cell dimensions	a = 11.5716(4) Å	α= 83.9090(10)°.
	b = 11.7964(4) Å	β= 82.6920(10)°.
	c = 12.7235(5) Å	γ = 75.7020(10)°.
Volume	1664.28(10) Å^3	
Z	2	
Density (calculated)	1.378 Mg/m^3	
Absorption coefficient	0.750 mm^{-1}	
F(000)	708	
Crystal size	0.50 x 0.43 x 0.25 mm^3	
Theta range for data collection	2.946 to 26.372°.	
Index ranges	-13<=h<=14, -14<=k<=14, -15<=l<=15	
Reflections collected	54027	
Independent reflections	6776 [R(int) = 0.1102]	
Completeness to theta = 26.000°	99.8 %	
Absorption correction	Semi-empirical from equivalents	
Max. and min. transmission	0.7456 and 0.6944	
Refinement method	Full-matrix least-squares on F^2	
Data / restraints / parameters	6776 / 130 / 368	
Goodness-of-fit on F^2	1.017	
Final R indices [I>2sigma(I)]	R1 = 0.0425, wR2 = 0.0849	
R indices (all data)	R1 = 0.0717, wR2 = 0.0951	
Extinction coefficient	n/a	
Largest diff. peak and hole	0.574 and -0.380 e.Å^{-3}	

Table 2. Atomic coordinates (x 10^4) and equivalent isotropic displacement parameters ($Å^2$x 10^3) for rudppm. U(eq) is defined as one third of the trace of the orthogonalized U^{ij} tensor.

	x	y	z	U(eq)
Ru(1)	425(1)	3894(1)	3088(1)	30(1)
Cl(1)	2265(1)	4423(1)	3298(1)	46(1)
Cl(2)	726(1)	2545(1)	4638(1)	42(1)
P(1)	1597(1)	2264(1)	2225(1)	29(1)
P(2)	4135(1)	609(1)	1952(1)	34(1)
C(1)	-1528(3)	4174(3)	3507(3)	46(1)
C(2)	-1167(3)	5128(3)	3860(3)	43(1)
C(3)	-519(3)	5775(3)	3181(3)	44(1)
C(4)	-178(4)	5530(3)	2094(3)	46(1)
C(5)	-556(4)	4616(4)	1739(3)	50(1)
C(6)	-1239(3)	3946(4)	2433(3)	50(1)
C(7)	-2251(4)	3507(4)	4291(5)	67(1)
C(8)	-3535(5)	4267(5)	4451(7)	129(3)
C(9)	-2220(5)	2274(5)	4018(5)	90(2)
C(10)	531(5)	6260(4)	1377(4)	71(1)
C(11)	2131(3)	2571(3)	837(3)	36(1)
C(12)	2524(4)	3582(3)	573(3)	54(1)
C(13)	3037(5)	3819(4)	-446(4)	76(2)
C(14)	3141(5)	3044(5)	-1203(4)	75(2)
C(15)	2777(4)	2038(5)	-952(3)	63(1)
C(16)	2281(3)	1785(4)	61(3)	45(1)
C(17)	802(3)	1110(3)	2213(3)	37(1)
C(18)	-13(4)	1199(4)	1480(4)	54(1)
C(19)	-693(4)	385(5)	1526(5)	77(1)
C(20)	-582(5)	-532(5)	2295(5)	85(2)
C(21)	222(5)	-629(5)	3018(5)	83(2)
C(22)	910(4)	185(4)	2985(4)	57(1)
C(23)	2978(3)	1553(3)	2827(3)	34(1)
C(24)	5089(3)	1582(3)	1364(3)	41(1)
C(25)	5175(5)	2596(4)	1770(4)	72(1)
C(26)	5914(6)	3267(5)	1253(5)	103(2)
C(27)	6567(6)	2963(6)	318(5)	106(2)
C(28)	6521(5)	1960(5)	-99(4)	85(2)

C(29)	5775(4)	1272(4)	419(3)	57(1)
C(30)	5030(3)	-303(3)	2961(3)	39(1)
C(31)	5970(4)	-38(4)	3364(3)	58(1)
C(32)	6631(5)	-823(5)	4080(4)	75(1)
C(33)	6363(5)	-1853(5)	4402(4)	70(1)
C(34)	5444(5)	-2136(5)	4026(4)	82(2)
C(35)	4774(4)	-1362(4)	3295(4)	64(1)

Table 3. Bond lengths [a] and angles [g] for rudppm.

Ru(1)-C(5)	2.161(4)
Ru(1)-C(6)	2.178(4)
Ru(1)-C(4)	2.202(4)
Ru(1)-C(1)	2.205(4)
Ru(1)-C(3)	2.226(3)
Ru(1)-C(2)	2.235(3)
Ru(1)-P(1)	2.3500(8)
Ru(1)-Cl(2)	2.4040(9)
Ru(1)-Cl(1)	2.4150(9)
P(1)-C(17)	1.823(4)
P(1)-C(11)	1.825(3)
P(1)-C(23)	1.832(3)
P(2)-C(24)	1.825(4)
P(2)-C(30)	1.836(4)
P(2)-C(23)	1.850(3)
C(1)-C(6)	1.403(5)
C(1)-C(2)	1.424(5)
C(1)-C(7)	1.504(6)
C(2)-C(3)	1.367(5)
C(2)-H(2)	0.9300
C(3)-C(4)	1.428(5)
C(3)-H(3)	0.9300
C(4)-C(5)	1.394(6)
C(4)-C(10)	1.497(6)
C(5)-C(6)	1.419(6)
C(5)-H(5)	0.9300
C(6)-H(6)	0.9300
C(7)-C(9)	1.521(7)
C(7)-C(8)	1.535(7)
C(7)-H(7)	0.92(4)
C(8)-H(8A)	0.9600
C(8)-H(8B)	0.9600
C(8)-H(8C)	0.9600
C(9)-H(9A)	0.9600
C(9)-H(9B)	0.9600
C(9)-H(9C)	0.9600

C(10)-H(10A)	0.9600
C(10)-H(10B)	0.9600
C(10)-H(10C)	0.9600
C(11)-C(12)	1.374(5)
C(11)-C(16)	1.390(5)
C(12)-C(13)	1.386(5)
C(12)-H(12)	0.9300
C(13)-C(14)	1.371(7)
C(13)-H(13)	0.9300
C(14)-C(15)	1.349(7)
C(14)-H(14)	0.9300
C(15)-C(16)	1.376(6)
C(15)-H(15)	0.9300
C(16)-H(16)	0.9300
C(17)-C(22)	1.381(5)
C(17)-C(18)	1.388(5)
C(18)-C(19)	1.377(6)
C(18)-H(18)	0.9300
C(19)-C(20)	1.372(8)
C(19)-H(19)	0.9300
C(20)-C(21)	1.367(8)
C(20)-H(20)	0.9300
C(21)-C(22)	1.385(6)
C(21)-H(21)	0.9300
C(22)-H(22)	0.9300
C(23)-H(23A)	0.9700
C(23)-H(23B)	0.9700
C(24)-C(25)	1.382(6)
C(24)-C(29)	1.385(5)
C(25)-C(26)	1.368(6)
C(25)-H(25)	0.9300
C(26)-C(27)	1.357(8)
C(26)-H(26)	0.9300
C(27)-C(28)	1.362(8)
C(27)-H(27)	0.9300
C(28)-C(29)	1.388(6)
C(28)-H(28)	0.9300
C(29)-H(29)	0.9300

C(30)-C(35)	1.365(6)
C(30)-C(31)	1.375(5)
C(31)-C(32)	1.386(6)
C(31)-H(31)	0.9300
C(32)-C(33)	1.337(7)
C(32)-H(32)	0.9300
C(33)-C(34)	1.346(7)
C(33)-H(33)	0.9300
C(34)-C(35)	1.398(6)
C(34)-H(34)	0.9300
C(35)-H(35)	0.9300

C(5)-Ru(1)-C(6)	38.18(16)
C(5)-Ru(1)-C(4)	37.25(15)
C(6)-Ru(1)-C(4)	68.06(16)
C(5)-Ru(1)-C(1)	68.24(16)
C(6)-Ru(1)-C(1)	37.34(14)
C(4)-Ru(1)-C(1)	80.67(15)
C(5)-Ru(1)-C(3)	66.69(14)
C(6)-Ru(1)-C(3)	78.57(15)
C(4)-Ru(1)-C(3)	37.62(13)
C(1)-Ru(1)-C(3)	66.47(15)
C(5)-Ru(1)-C(2)	78.86(14)
C(6)-Ru(1)-C(2)	66.63(14)
C(4)-Ru(1)-C(2)	66.81(14)
C(1)-Ru(1)-C(2)	37.40(14)
C(3)-Ru(1)-C(2)	35.70(14)
C(5)-Ru(1)-P(1)	94.00(10)
C(6)-Ru(1)-P(1)	96.63(10)
C(4)-Ru(1)-P(1)	117.35(10)
C(1)-Ru(1)-P(1)	123.25(10)
C(3)-Ru(1)-P(1)	154.57(10)
C(2)-Ru(1)-P(1)	160.65(10)
C(5)-Ru(1)-Cl(2)	150.26(13)
C(6)-Ru(1)-Cl(2)	112.63(12)
C(4)-Ru(1)-Cl(2)	160.19(10)
C(1)-Ru(1)-Cl(2)	89.00(11)
C(3)-Ru(1)-Cl(2)	122.60(10)

C(2)-Ru(1)-Cl(2)	94.81(10)
P(1)-Ru(1)-Cl(2)	82.45(3)
C(5)-Ru(1)-Cl(1)	120.70(13)
C(6)-Ru(1)-Cl(1)	158.49(12)
C(4)-Ru(1)-Cl(1)	91.16(11)
C(1)-Ru(1)-Cl(1)	148.19(11)
C(3)-Ru(1)-Cl(1)	88.36(11)
C(2)-Ru(1)-Cl(1)	111.31(10)
P(1)-Ru(1)-Cl(1)	87.85(3)
Cl(2)-Ru(1)-Cl(1)	88.78(3)
C(17)-P(1)-C(11)	105.06(16)
C(17)-P(1)-C(23)	105.44(16)
C(11)-P(1)-C(23)	103.22(16)
C(17)-P(1)-Ru(1)	112.73(11)
C(11)-P(1)-Ru(1)	115.37(11)
C(23)-P(1)-Ru(1)	113.95(11)
C(24)-P(2)-C(30)	102.57(17)
C(24)-P(2)-C(23)	103.30(16)
C(30)-P(2)-C(23)	99.54(15)
C(6)-C(1)-C(2)	118.1(4)
C(6)-C(1)-C(7)	123.5(4)
C(2)-C(1)-C(7)	118.3(4)
C(6)-C(1)-Ru(1)	70.3(2)
C(2)-C(1)-Ru(1)	72.5(2)
C(7)-C(1)-Ru(1)	131.1(3)
C(3)-C(2)-C(1)	120.9(4)
C(3)-C(2)-Ru(1)	71.8(2)
C(1)-C(2)-Ru(1)	70.1(2)
C(3)-C(2)-H(2)	119.5
C(1)-C(2)-H(2)	119.5
Ru(1)-C(2)-H(2)	131.4
C(2)-C(3)-C(4)	121.8(4)
C(2)-C(3)-Ru(1)	72.5(2)
C(4)-C(3)-Ru(1)	70.3(2)
C(2)-C(3)-H(3)	119.1
C(4)-C(3)-H(3)	119.1
Ru(1)-C(3)-H(3)	131.0
C(5)-C(4)-C(3)	117.4(4)

C(5)-C(4)-C(10)	122.4(4)
C(3)-C(4)-C(10)	120.2(4)
C(5)-C(4)-Ru(1)	69.7(2)
C(3)-C(4)-Ru(1)	72.1(2)
C(10)-C(4)-Ru(1)	130.3(3)
C(4)-C(5)-C(6)	121.2(4)
C(4)-C(5)-Ru(1)	73.0(2)
C(6)-C(5)-Ru(1)	71.6(2)
C(4)-C(5)-H(5)	119.4
C(6)-C(5)-H(5)	119.4
Ru(1)-C(5)-H(5)	128.3
C(1)-C(6)-C(5)	120.4(4)
C(1)-C(6)-Ru(1)	72.4(2)
C(5)-C(6)-Ru(1)	70.3(2)
C(1)-C(6)-H(6)	119.8
C(5)-C(6)-H(6)	119.8
Ru(1)-C(6)-H(6)	130.1
C(1)-C(7)-C(9)	115.3(4)
C(1)-C(7)-C(8)	108.0(4)
C(9)-C(7)-C(8)	112.3(5)
C(1)-C(7)-H(7)	110(3)
C(9)-C(7)-H(7)	102(3)
C(8)-C(7)-H(7)	109(3)
C(7)-C(8)-H(8A)	109.5
C(7)-C(8)-H(8B)	109.5
H(8A)-C(8)-H(8B)	109.5
C(7)-C(8)-H(8C)	109.5
H(8A)-C(8)-H(8C)	109.5
H(8B)-C(8)-H(8C)	109.5
C(7)-C(9)-H(9A)	109.5
C(7)-C(9)-H(9B)	109.5
H(9A)-C(9)-H(9B)	109.5
C(7)-C(9)-H(9C)	109.5
H(9A)-C(9)-H(9C)	109.5
H(9B)-C(9)-H(9C)	109.5
C(4)-C(10)-H(10A)	109.5
C(4)-C(10)-H(10B)	109.5
H(10A)-C(10)-H(10B)	109.5

C(4)-C(10)-H(10C)	109.5
H(10A)-C(10)-H(10C)	109.5
H(10B)-C(10)-H(10C)	109.5
C(12)-C(11)-C(16)	118.3(3)
C(12)-C(11)-P(1)	117.7(3)
C(16)-C(11)-P(1)	123.7(3)
C(11)-C(12)-C(13)	120.6(4)
C(11)-C(12)-H(12)	119.7
C(13)-C(12)-H(12)	119.7
C(14)-C(13)-C(12)	119.8(5)
C(14)-C(13)-H(13)	120.1
C(12)-C(13)-H(13)	120.1
C(15)-C(14)-C(13)	120.3(4)
C(15)-C(14)-H(14)	119.8
C(13)-C(14)-H(14)	119.8
C(14)-C(15)-C(16)	120.4(4)
C(14)-C(15)-H(15)	119.8
C(16)-C(15)-H(15)	119.8
C(15)-C(16)-C(11)	120.5(4)
C(15)-C(16)-H(16)	119.7
C(11)-C(16)-H(16)	119.7
C(22)-C(17)-C(18)	118.1(4)
C(22)-C(17)-P(1)	121.3(3)
C(18)-C(17)-P(1)	120.3(3)
C(19)-C(18)-C(17)	120.6(5)
C(19)-C(18)-H(18)	119.7
C(17)-C(18)-H(18)	119.7
C(20)-C(19)-C(18)	121.0(5)
C(20)-C(19)-H(19)	119.5
C(18)-C(19)-H(19)	119.5
C(21)-C(20)-C(19)	118.9(5)
C(21)-C(20)-H(20)	120.6
C(19)-C(20)-H(20)	120.6
C(20)-C(21)-C(22)	120.9(5)
C(20)-C(21)-H(21)	119.5
C(22)-C(21)-H(21)	119.5
C(17)-C(22)-C(21)	120.5(5)
C(17)-C(22)-H(22)	119.7

C(21)-C(22)-H(22)	119.7
P(1)-C(23)-P(2)	114.74(17)
P(1)-C(23)-H(23A)	108.6
P(2)-C(23)-H(23A)	108.6
P(1)-C(23)-H(23B)	108.6
P(2)-C(23)-H(23B)	108.6
H(23A)-C(23)-H(23B)	107.6
C(25)-C(24)-C(29)	117.7(4)
C(25)-C(24)-P(2)	126.0(3)
C(29)-C(24)-P(2)	116.3(3)
C(26)-C(25)-C(24)	121.0(5)
C(26)-C(25)-H(25)	119.5
C(24)-C(25)-H(25)	119.5
C(27)-C(26)-C(25)	120.7(5)
C(27)-C(26)-H(26)	119.6
C(25)-C(26)-H(26)	119.6
C(26)-C(27)-C(28)	120.0(5)
C(26)-C(27)-H(27)	120.0
C(28)-C(27)-H(27)	120.0
C(27)-C(28)-C(29)	119.7(5)
C(27)-C(28)-H(28)	120.1
C(29)-C(28)-H(28)	120.1
C(24)-C(29)-C(28)	120.8(4)
C(24)-C(29)-H(29)	119.6
C(28)-C(29)-H(29)	119.6
C(35)-C(30)-C(31)	117.5(4)
C(35)-C(30)-P(2)	116.8(3)
C(31)-C(30)-P(2)	125.6(3)
C(30)-C(31)-C(32)	120.8(4)
C(30)-C(31)-H(31)	119.6
C(32)-C(31)-H(31)	119.6
C(33)-C(32)-C(31)	120.8(5)
C(33)-C(32)-H(32)	119.6
C(31)-C(32)-H(32)	119.6
C(32)-C(33)-C(34)	119.8(5)
C(32)-C(33)-H(33)	120.1
C(34)-C(33)-H(33)	120.1
C(33)-C(34)-C(35)	120.2(5)

C(33)-C(34)-H(34)	119.9
C(35)-C(34)-H(34)	119.9
C(30)-C(35)-C(34)	120.8(4)
C(30)-C(35)-H(35)	119.6
C(34)-C(35)-H(35)	119.6

Symmetry transformations used to generate equivalent atoms:

Table 4. Anisotropic displacement parameters ($Å^2$x 10^3)for rudppm. The anisotropic displacement factor exponent takes the form: $-2\pi^2[h^2a^{*2}U^{11} + ... + 2 h k a^* b^* U^{12}]$

	U^{11}	U^{22}	U^{33}	U^{23}	U^{13}	U^{12}
Ru(1)	30(1)	32(1)	26(1)	-8(1)	-1(1)	-2(1)
Cl(1)	42(1)	49(1)	52(1)	-16(1)	0(1)	-16(1)
Cl(2)	45(1)	47(1)	29(1)	0(1)	-1(1)	-4(1)
P(1)	30(1)	29(1)	26(1)	-6(1)	-2(1)	-2(1)
P(2)	30(1)	36(1)	35(1)	-9(1)	-3(1)	-2(1)
C(1)	24(2)	45(2)	62(2)	-12(2)	-1(2)	5(2)
C(2)	37(2)	45(2)	41(2)	-14(2)	2(2)	4(2)
C(3)	48(2)	32(2)	45(2)	-11(2)	-2(2)	4(2)
C(4)	51(2)	38(2)	37(2)	-1(2)	-6(2)	9(2)
C(5)	50(2)	54(2)	37(2)	-11(2)	-15(2)	13(2)
C(6)	32(2)	50(2)	66(3)	-25(2)	-21(2)	9(2)
C(7)	40(3)	59(3)	95(4)	-14(3)	14(3)	-8(2)
C(8)	45(3)	91(4)	233(9)	-30(5)	49(4)	-6(3)
C(9)	63(3)	72(3)	139(5)	-20(3)	18(3)	-31(3)
C(10)	91(4)	48(3)	55(3)	8(2)	8(2)	5(2)
C(11)	35(2)	37(2)	31(2)	-5(2)	-2(1)	3(2)
C(12)	70(3)	38(2)	44(2)	-6(2)	14(2)	-4(2)
C(13)	95(4)	53(3)	61(3)	11(2)	28(3)	-7(3)
C(14)	79(4)	83(4)	38(2)	6(2)	15(2)	11(3)
C(15)	59(3)	85(3)	37(2)	-23(2)	-1(2)	6(2)
C(16)	42(2)	52(2)	38(2)	-15(2)	-2(2)	1(2)
C(17)	35(2)	37(2)	41(2)	-12(2)	-1(2)	-7(2)
C(18)	47(3)	54(3)	64(3)	-17(2)	-9(2)	-13(2)
C(19)	61(3)	81(4)	101(4)	-38(3)	-15(3)	-25(3)
C(20)	71(4)	71(4)	126(5)	-32(3)	8(3)	-40(3)
C(21)	98(4)	52(3)	104(4)	2(3)	0(3)	-33(3)
C(22)	62(3)	45(2)	67(3)	0(2)	-6(2)	-19(2)
C(23)	30(2)	38(2)	31(2)	-5(2)	-2(1)	-3(2)
C(24)	34(2)	43(2)	42(2)	-5(2)	0(2)	-5(2)
C(25)	82(4)	67(3)	73(3)	-22(2)	27(3)	-39(3)
C(26)	116(5)	83(4)	121(5)	-31(4)	41(4)	-62(4)
C(27)	107(5)	104(5)	115(5)	-9(4)	43(4)	-68(4)
C(28)	80(4)	105(4)	69(3)	-12(3)	28(3)	-36(3)

C(29)	52(3)	65(3)	51(2)	-8(2)	9(2)	-11(2)
C(30)	32(2)	37(2)	41(2)	-7(2)	1(2)	2(2)
C(31)	57(3)	57(3)	61(3)	-2(2)	-22(2)	-13(2)
C(32)	71(4)	86(4)	68(3)	-3(3)	-33(3)	-6(3)
C(33)	59(3)	79(3)	54(3)	4(2)	-10(2)	15(3)
C(34)	78(4)	61(3)	95(4)	31(3)	-14(3)	-9(3)
C(35)	51(3)	57(3)	83(3)	14(2)	-16(2)	-16(2)

Table 5. Hydrogen coordinates (x 10^4) and isotropic displacement parameters ($Å^2$x 10^3) for rudppm.

	x	y	z	U(eq)
H(2)	-1375	5313	4562	52
H(3)	-295	6392	3433	52
H(5)	-356	4442	1033	60
H(6)	-1496	3352	2175	60
H(7)	-1930(40)	3360(40)	4930(30)	55(14)
H(8A)	-3511	5051	4567	194
H(8B)	-3966	3943	5057	194
H(8C)	-3933	4281	3831	194
H(9A)	-2561	2316	3361	136
H(9B)	-2674	1905	4575	136
H(9C)	-1405	1824	3945	136
H(10A)	1182	6357	1730	106
H(10B)	22	7015	1203	106
H(10C)	845	5876	737	106
H(12)	2445	4114	1083	65
H(13)	3310	4501	-617	91
H(14)	3465	3212	-1892	90
H(15)	2861	1511	-1467	76
H(16)	2045	1084	229	55
H(18)	-101	1814	952	65
H(19)	-1235	457	1028	92
H(20)	-1047	-1077	2324	102
H(21)	309	-1251	3539	100
H(22)	1448	109	3487	69
H(23A)	2776	1081	3463	41
H(23B)	3316	2157	3043	41
H(25)	4724	2826	2403	87
H(26)	5970	3939	1545	123
H(27)	7046	3440	-38	127
H(28)	6987	1738	-727	102
H(29)	5735	594	127	69
H(31)	6165	677	3154	69

H(32)	7269	-631	4340	90
H(33)	6811	-2372	4885	84
H(34)	5254	-2850	4253	98
H(35)	4147	-1570	3033	77

Table 6. Torsion angles [°] for rudppm.

C(6)-C(1)-C(2)-C(3)	-2.4(5)
C(7)-C(1)-C(2)-C(3)	-179.3(4)
Ru(1)-C(1)-C(2)-C(3)	52.9(3)
C(6)-C(1)-C(2)-Ru(1)	-55.3(3)
C(7)-C(1)-C(2)-Ru(1)	127.8(4)
C(1)-C(2)-C(3)-C(4)	0.1(6)
Ru(1)-C(2)-C(3)-C(4)	52.3(3)
C(1)-C(2)-C(3)-Ru(1)	-52.1(3)
C(2)-C(3)-C(4)-C(5)	1.5(5)
Ru(1)-C(3)-C(4)-C(5)	54.7(3)
C(2)-C(3)-C(4)-C(10)	180.0(4)
Ru(1)-C(3)-C(4)-C(10)	-126.8(4)
C(2)-C(3)-C(4)-Ru(1)	-53.2(3)
C(3)-C(4)-C(5)-C(6)	-0.8(5)
C(10)-C(4)-C(5)-C(6)	-179.3(4)
Ru(1)-C(4)-C(5)-C(6)	55.1(3)
C(3)-C(4)-C(5)-Ru(1)	-55.9(3)
C(10)-C(4)-C(5)-Ru(1)	125.6(4)
C(2)-C(1)-C(6)-C(5)	3.0(5)
C(7)-C(1)-C(6)-C(5)	179.7(4)
Ru(1)-C(1)-C(6)-C(5)	-53.3(3)
C(2)-C(1)-C(6)-Ru(1)	56.3(3)
C(7)-C(1)-C(6)-Ru(1)	-126.9(4)
C(4)-C(5)-C(6)-C(1)	-1.4(6)
Ru(1)-C(5)-C(6)-C(1)	54.3(3)
C(4)-C(5)-C(6)-Ru(1)	-55.8(3)
C(6)-C(1)-C(7)-C(9)	24.8(7)
C(2)-C(1)-C(7)-C(9)	-158.5(4)
Ru(1)-C(1)-C(7)-C(9)	-67.6(6)
C(6)-C(1)-C(7)-C(8)	-101.7(5)
C(2)-C(1)-C(7)-C(8)	75.0(6)
Ru(1)-C(1)-C(7)-C(8)	165.9(4)
C(17)-P(1)-C(11)-C(12)	165.5(3)
C(23)-P(1)-C(11)-C(12)	-84.3(3)
Ru(1)-P(1)-C(11)-C(12)	40.7(3)
C(17)-P(1)-C(11)-C(16)	-21.6(3)

C(23)-P(1)-C(11)-C(16)	88.6(3)
Ru(1)-P(1)-C(11)-C(16)	-146.4(3)
C(16)-C(11)-C(12)-C(13)	1.1(6)
P(1)-C(11)-C(12)-C(13)	174.4(4)
C(11)-C(12)-C(13)-C(14)	0.8(7)
C(12)-C(13)-C(14)-C(15)	-1.8(8)
C(13)-C(14)-C(15)-C(16)	0.9(7)
C(14)-C(15)-C(16)-C(11)	1.0(6)
C(12)-C(11)-C(16)-C(15)	-2.0(6)
P(1)-C(11)-C(16)-C(15)	-174.9(3)
C(11)-P(1)-C(17)-C(22)	139.3(3)
C(23)-P(1)-C(17)-C(22)	30.6(3)
Ru(1)-P(1)-C(17)-C(22)	-94.3(3)
C(11)-P(1)-C(17)-C(18)	-46.6(3)
C(23)-P(1)-C(17)-C(18)	-155.3(3)
Ru(1)-P(1)-C(17)-C(18)	79.8(3)
C(22)-C(17)-C(18)-C(19)	0.0(6)
P(1)-C(17)-C(18)-C(19)	-174.2(3)
C(17)-C(18)-C(19)-C(20)	0.0(7)
C(18)-C(19)-C(20)-C(21)	-0.3(8)
C(19)-C(20)-C(21)-C(22)	0.5(9)
C(18)-C(17)-C(22)-C(21)	0.2(6)
P(1)-C(17)-C(22)-C(21)	174.4(4)
C(20)-C(21)-C(22)-C(17)	-0.5(8)
C(17)-P(1)-C(23)-P(2)	74.9(2)
C(11)-P(1)-C(23)-P(2)	-35.1(2)
Ru(1)-P(1)-C(23)-P(2)	-160.98(13)
C(24)-P(2)-C(23)-P(1)	94.8(2)
C(30)-P(2)-C(23)-P(1)	-159.7(2)
C(30)-P(2)-C(24)-C(25)	-82.3(4)
C(23)-P(2)-C(24)-C(25)	20.9(4)
C(30)-P(2)-C(24)-C(29)	98.6(3)
C(23)-P(2)-C(24)-C(29)	-158.3(3)
C(29)-C(24)-C(25)-C(26)	-0.1(8)
P(2)-C(24)-C(25)-C(26)	-179.3(5)
C(24)-C(25)-C(26)-C(27)	1.1(11)
C(25)-C(26)-C(27)-C(28)	-2.2(12)
C(26)-C(27)-C(28)-C(29)	2.1(11)

C(25)-C(24)-C(29)-C(28)	0.1(7)
P(2)-C(24)-C(29)-C(28)	179.3(4)
C(27)-C(28)-C(29)-C(24)	-1.1(9)
C(24)-P(2)-C(30)-C(35)	-158.4(3)
C(23)-P(2)-C(30)-C(35)	95.5(3)
C(24)-P(2)-C(30)-C(31)	17.9(4)
C(23)-P(2)-C(30)-C(31)	-88.1(4)
C(35)-C(30)-C(31)-C(32)	0.2(6)
P(2)-C(30)-C(31)-C(32)	-176.2(4)
C(30)-C(31)-C(32)-C(33)	-0.5(8)
C(31)-C(32)-C(33)-C(34)	0.2(8)
C(32)-C(33)-C(34)-C(35)	0.4(8)
C(31)-C(30)-C(35)-C(34)	0.5(7)
P(2)-C(30)-C(35)-C(34)	177.1(4)
C(33)-C(34)-C(35)-C(30)	-0.8(8)

Symmetry transformations used to generate equivalent atoms:

Table 7. Hydrogen bonds for rudppm [a and g].

D-H...A	d(D-H)	d(H...A)	d(D...A)	<(DHA)
C(23)-H(23B)...Cl(1)	0.97	2.68	3.380(4)	128.9
C(12)-H(12)...Cl(1)	0.93	2.86	3.663(4)	145.9
C(2)-H(2)...Cl(1)#1	0.93	2.81	3.725(4)	170.0
C(3)-H(3)...Cl(2)#1	0.93	0.81	3.529(4)	135.0

Symmetry transformations used to generate equivalent atoms: #1 -x,-y+1,-z+1

Supplementary data

Characterization of [Ru(*p*-cymene)(tbp)Cl_2] complex

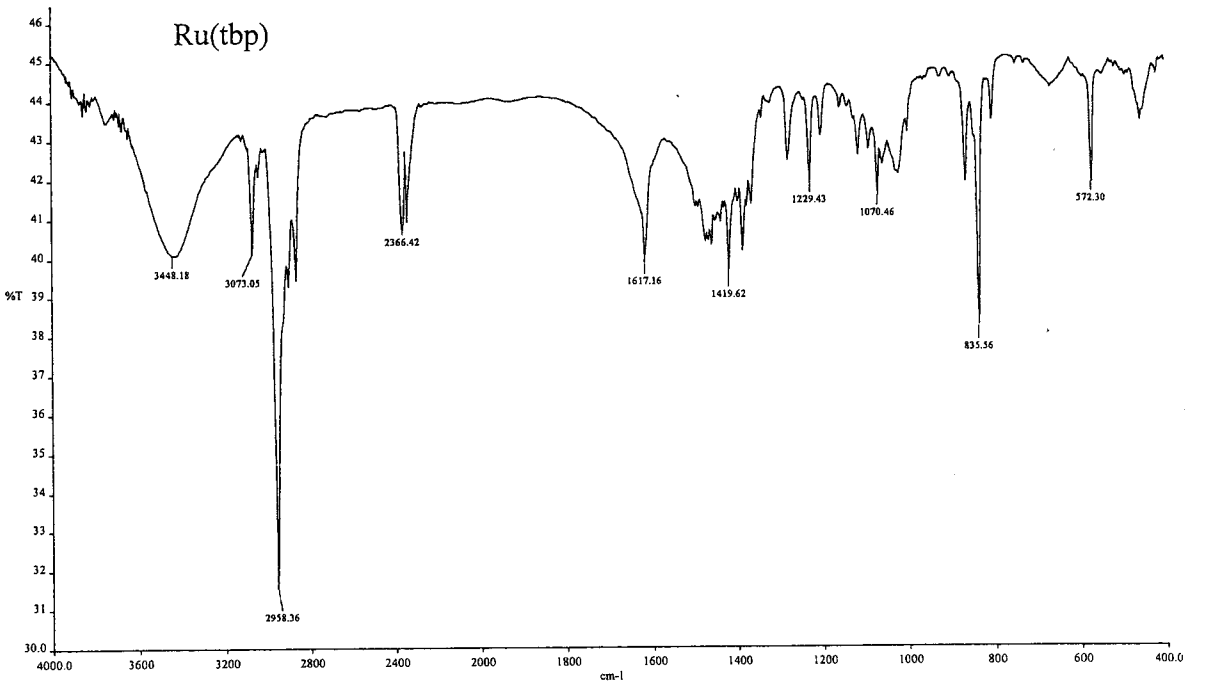

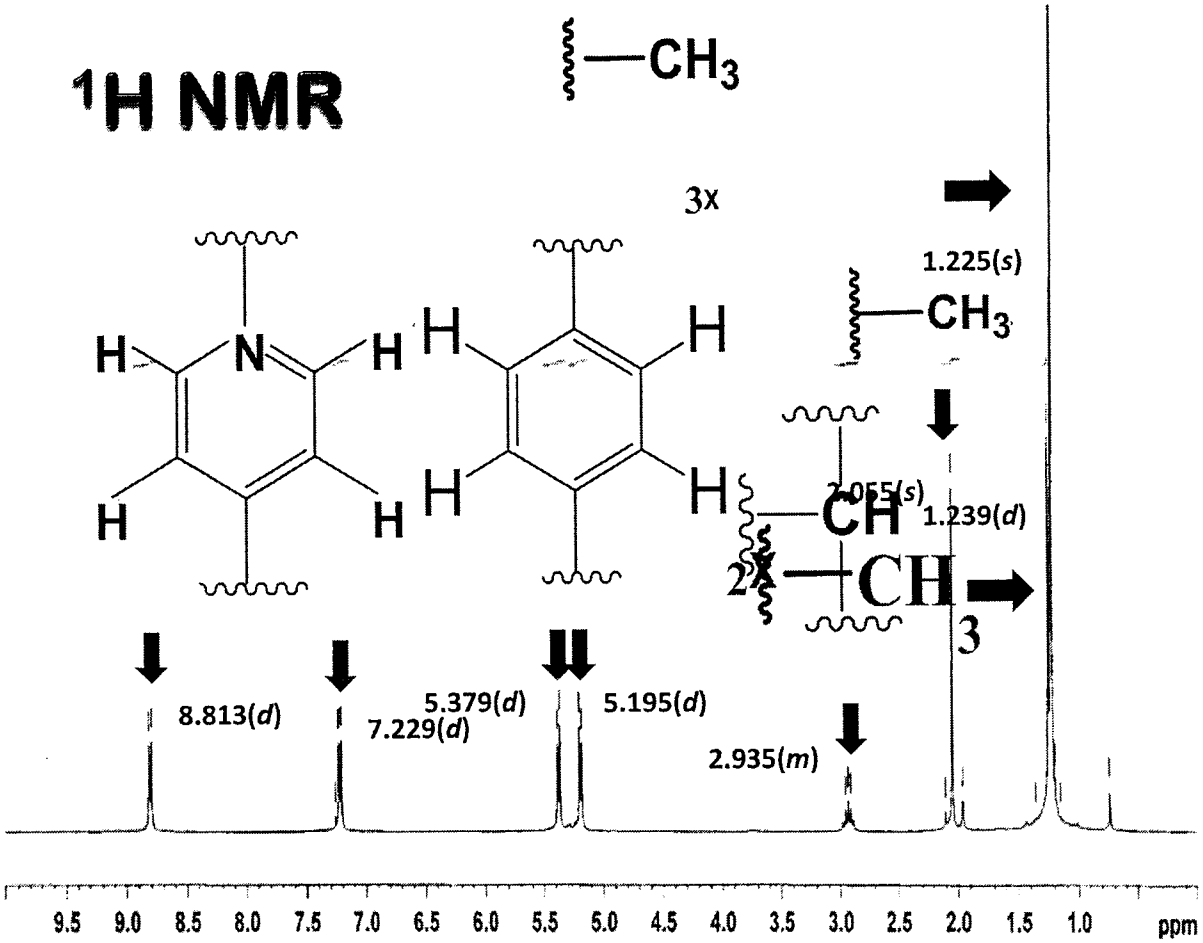
1H NMR
CH3
3x
1.225(s)
CH3
H
N
H
H
H
H
H
H
H
2.055(s)
1.239(d)
CH
2x
CH
3
8.813(d)
7.229(d)
5.379(d)
5.195(d)
2.935(m)
9.5
9.0
8.5
8.0
7.5
7.0
6.5
6.0
5.5
5.0
4.5
4.0
3.5
3.0
2.5
2.0
1.5
1.0
ppm

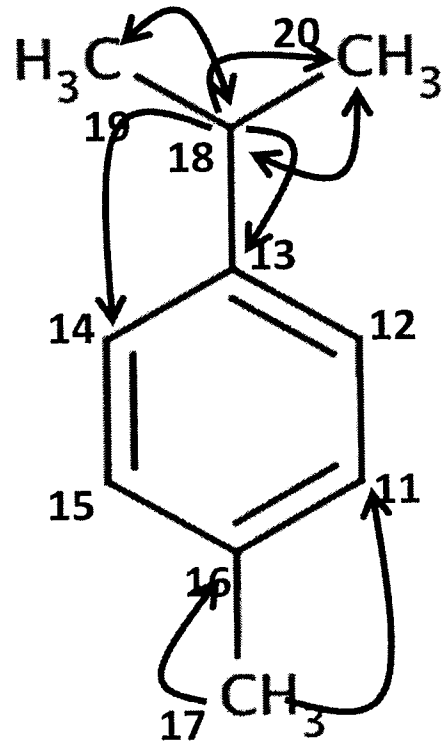

COSY

HMBC

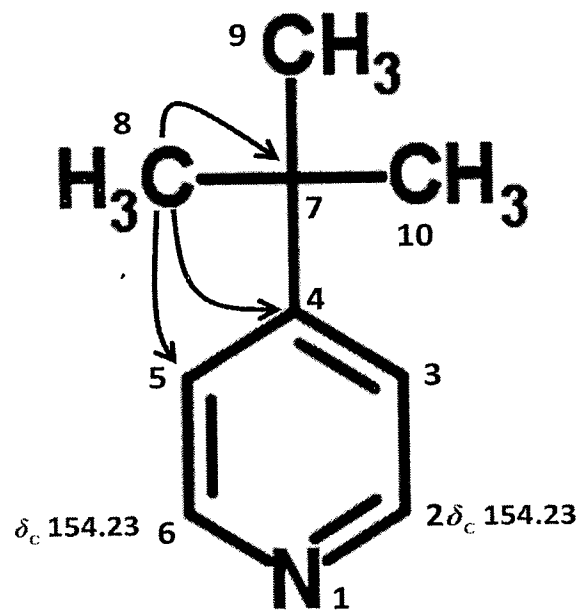

COSY

HMBC

Complex	Elemental analysis (%)					
	Calculated			Found		
	C	H	N	C	H	N
Ru(tbp)	51.70	6.17	3.17	51.48±0.16	6.28±0.05	3.13±0.09

Supplementary data

Characterization of [Ru(*p*-cymene)(dppm)Cl_2] complex

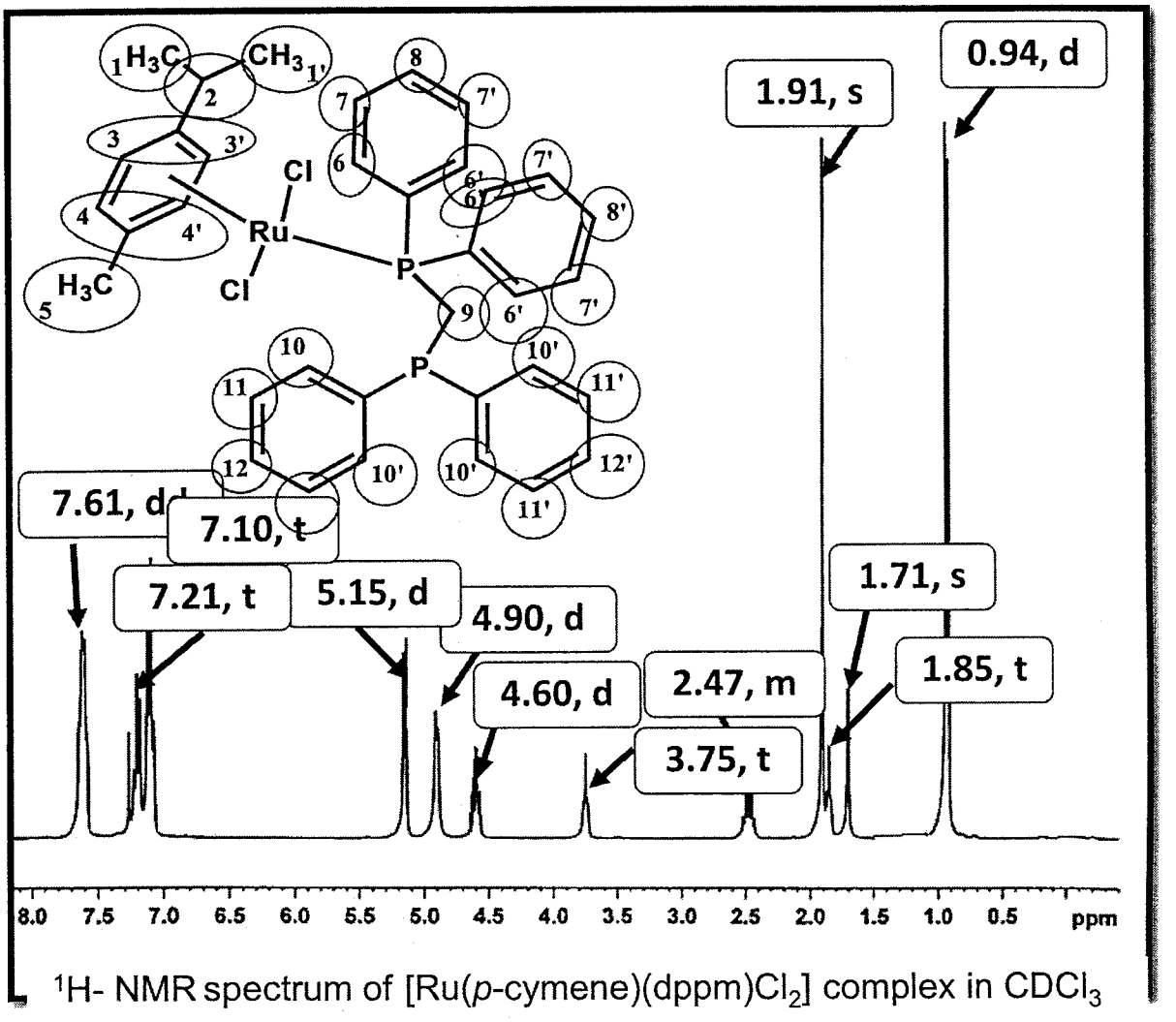

^{1}H- NMR spectrum of [Ru(*p*-cymene)(dppm)Cl_2] complex in $CDCl_3$

Investigate	% Element (SD)		
	%N	% C	% H
Calcd.	-	60.87	6.02
Found	-	60.21(2.17×10^{-2})	6.22(3.09×10^{-2})

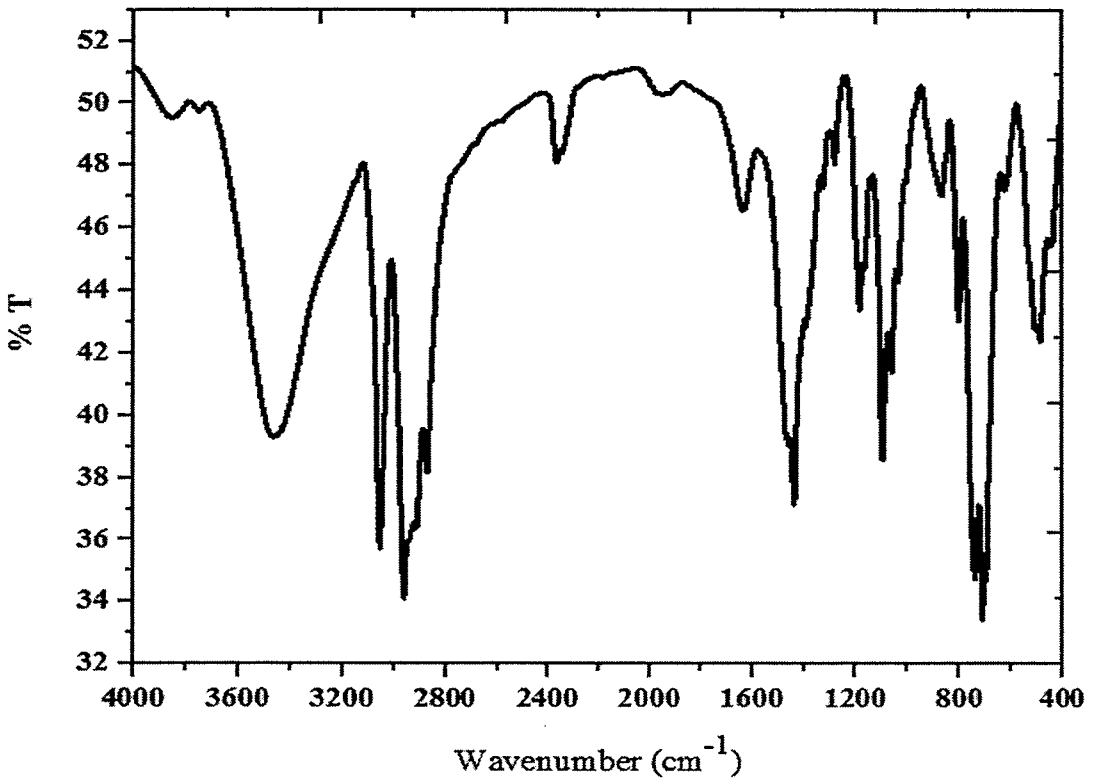

IR spectrum of [Ru(*p*-cymene)(dppm)Cl_2], Ru(dppm) complex.

Table 1. Crystal data and structure refinement for rudppm.

Identification code	shelx	
Empirical formula	C35 H36 Cl2 P2 Ru	
Formula weight	690.55	
Temperature	293(2) K	
Wavelength	0.71073 Å	
Crystal system	Triclinic	
Space group	P -1	
Unit cell dimensions	a = 11.5716(4) Å	α= 83.9090(10)°.
	b = 11.7964(4) Å	β= 82.6920(10)°.
	c = 12.7235(5) Å	γ = 75.7020(10)°.
Volume	1664.28(10) Å^3	
Z	2	
Density (calculated)	1.378 Mg/m^3	
Absorption coefficient	0.750 mm^{-1}	
F(000)	708	
Crystal size	0.50 x 0.43 x 0.25 mm^3	
Theta range for data collection	2.946 to 26.372°.	
Index ranges	-13<=h<=14, -14<=k<=14, -15<=l<=15	
Reflections collected	54027	
Independent reflections	6776 [R(int) = 0.1102]	
Completeness to theta = 26.000°	99.8 %	
Absorption correction	Semi-empirical from equivalents	
Max. and min. transmission	0.7456 and 0.6944	
Refinement method	Full-matrix least-squares on F^2	
Data / restraints / parameters	6776 / 130 / 368	
Goodness-of-fit on F^2	1.017	
Final R indices [I>2sigma(I)]	R1 = 0.0425, wR2 = 0.0849	
R indices (all data)	R1 = 0.0717, wR2 = 0.0951	
Extinction coefficient	n/a	
Largest diff. peak and hole	0.574 and -0.380 e.Å^{-3}	

Table 2. Atomic coordinates (x 10^4) and equivalent isotropic displacement parameters ($Å^2$x 10^3) for rudppm. U(eq) is defined as one third of the trace of the orthogonalized U^{ij} tensor.

	x	y	z	U(eq)
Ru(1)	425(1)	3894(1)	3088(1)	30(1)
Cl(1)	2265(1)	4423(1)	3298(1)	46(1)
Cl(2)	726(1)	2545(1)	4638(1)	42(1)
P(1)	1597(1)	2264(1)	2225(1)	29(1)
P(2)	4135(1)	609(1)	1952(1)	34(1)
C(1)	-1528(3)	4174(3)	3507(3)	46(1)
C(2)	-1167(3)	5128(3)	3860(3)	43(1)
C(3)	-519(3)	5775(3)	3181(3)	44(1)
C(4)	-178(4)	5530(3)	2094(3)	46(1)
C(5)	-556(4)	4616(4)	1739(3)	50(1)
C(6)	-1239(3)	3946(4)	2433(3)	50(1)
C(7)	-2251(4)	3507(4)	4291(5)	67(1)
C(8)	-3535(5)	4267(5)	4451(7)	129(3)
C(9)	-2220(5)	2274(5)	4018(5)	90(2)
C(10)	531(5)	6260(4)	1377(4)	71(1)
C(11)	2131(3)	2571(3)	837(3)	36(1)
C(12)	2524(4)	3582(3)	573(3)	54(1)
C(13)	3037(5)	3819(4)	-446(4)	76(2)
C(14)	3141(5)	3044(5)	-1203(4)	75(2)
C(15)	2777(4)	2038(5)	-952(3)	63(1)
C(16)	2281(3)	1785(4)	61(3)	45(1)
C(17)	802(3)	1110(3)	2213(3)	37(1)
C(18)	-13(4)	1199(4)	1480(4)	54(1)
C(19)	-693(4)	385(5)	1526(5)	77(1)
C(20)	-582(5)	-532(5)	2295(5)	85(2)
C(21)	222(5)	-629(5)	3018(5)	83(2)
C(22)	910(4)	185(4)	2985(4)	57(1)
C(23)	2978(3)	1553(3)	2827(3)	34(1)
C(24)	5089(3)	1582(3)	1364(3)	41(1)
C(25)	5175(5)	2596(4)	1770(4)	72(1)
C(26)	5914(6)	3267(5)	1253(5)	103(2)
C(27)	6567(6)	2963(6)	318(5)	106(2)
C(28)	6521(5)	1960(5)	-99(4)	85(2)

C(29)	5775(4)	1272(4)	419(3)	57(1)
C(30)	5030(3)	-303(3)	2961(3)	39(1)
C(31)	5970(4)	-38(4)	3364(3)	58(1)
C(32)	6631(5)	-823(5)	4080(4)	75(1)
C(33)	6363(5)	-1853(5)	4402(4)	70(1)
C(34)	5444(5)	-2136(5)	4026(4)	82(2)
C(35)	4774(4)	-1362(4)	3295(4)	64(1)

Table 3. Bond lengths [å] and angles [°] for rudppm.

Ru(1)-C(5)	2.161(4)
Ru(1)-C(6)	2.178(4)
Ru(1)-C(4)	2.202(4)
Ru(1)-C(1)	2.205(4)
Ru(1)-C(3)	2.226(3)
Ru(1)-C(2)	2.235(3)
Ru(1)-P(1)	2.3500(8)
Ru(1)-Cl(2)	2.4040(9)
Ru(1)-Cl(1)	2.4150(9)
P(1)-C(17)	1.823(4)
P(1)-C(11)	1.825(3)
P(1)-C(23)	1.832(3)
P(2)-C(24)	1.825(4)
P(2)-C(30)	1.836(4)
P(2)-C(23)	1.850(3)
C(1)-C(6)	1.403(5)
C(1)-C(2)	1.424(5)
C(1)-C(7)	1.504(6)
C(2)-C(3)	1.367(5)
C(2)-H(2)	0.9300
C(3)-C(4)	1.428(5)
C(3)-H(3)	0.9300
C(4)-C(5)	1.394(6)
C(4)-C(10)	1.497(6)
C(5)-C(6)	1.419(6)
C(5)-H(5)	0.9300
C(6)-H(6)	0.9300
C(7)-C(9)	1.521(7)
C(7)-C(8)	1.535(7)
C(7)-H(7)	0.92(4)
C(8)-H(8A)	0.9600
C(8)-H(8B)	0.9600
C(8)-H(8C)	0.9600
C(9)-H(9A)	0.9600
C(9)-H(9B)	0.9600
C(9)-H(9C)	0.9600

C(10)-H(10A)	0.9600
C(10)-H(10B)	0.9600
C(10)-H(10C)	0.9600
C(11)-C(12)	1.374(5)
C(11)-C(16)	1.390(5)
C(12)-C(13)	1.386(5)
C(12)-H(12)	0.9300
C(13)-C(14)	1.371(7)
C(13)-H(13)	0.9300
C(14)-C(15)	1.349(7)
C(14)-H(14)	0.9300
C(15)-C(16)	1.376(6)
C(15)-H(15)	0.9300
C(16)-H(16)	0.9300
C(17)-C(22)	1.381(5)
C(17)-C(18)	1.388(5)
C(18)-C(19)	1.377(6)
C(18)-H(18)	0.9300
C(19)-C(20)	1.372(8)
C(19)-H(19)	0.9300
C(20)-C(21)	1.367(8)
C(20)-H(20)	0.9300
C(21)-C(22)	1.385(6)
C(21)-H(21)	0.9300
C(22)-H(22)	0.9300
C(23)-H(23A)	0.9700
C(23)-H(23B)	0.9700
C(24)-C(25)	1.382(6)
C(24)-C(29)	1.385(5)
C(25)-C(26)	1.368(6)
C(25)-H(25)	0.9300
C(26)-C(27)	1.357(8)
C(26)-H(26)	0.9300
C(27)-C(28)	1.362(8)
C(27)-H(27)	0.9300
C(28)-C(29)	1.388(6)
C(28)-H(28)	0.9300
C(29)-H(29)	0.9300

C(30)-C(35)	1.365(6)
C(30)-C(31)	1.375(5)
C(31)-C(32)	1.386(6)
C(31)-H(31)	0.9300
C(32)-C(33)	1.337(7)
C(32)-H(32)	0.9300
C(33)-C(34)	1.346(7)
C(33)-H(33)	0.9300
C(34)-C(35)	1.398(6)
C(34)-H(34)	0.9300
C(35)-H(35)	0.9300

C(5)-Ru(1)-C(6)	38.18(16)
C(5)-Ru(1)-C(4)	37.25(15)
C(6)-Ru(1)-C(4)	68.06(16)
C(5)-Ru(1)-C(1)	68.24(16)
C(6)-Ru(1)-C(1)	37.34(14)
C(4)-Ru(1)-C(1)	80.67(15)
C(5)-Ru(1)-C(3)	66.69(14)
C(6)-Ru(1)-C(3)	78.57(15)
C(4)-Ru(1)-C(3)	37.62(13)
C(1)-Ru(1)-C(3)	66.47(15)
C(5)-Ru(1)-C(2)	78.86(14)
C(6)-Ru(1)-C(2)	66.63(14)
C(4)-Ru(1)-C(2)	66.81(14)
C(1)-Ru(1)-C(2)	37.40(14)
C(3)-Ru(1)-C(2)	35.70(14)
C(5)-Ru(1)-P(1)	94.00(10)
C(6)-Ru(1)-P(1)	96.63(10)
C(4)-Ru(1)-P(1)	117.35(10)
C(1)-Ru(1)-P(1)	123.25(10)
C(3)-Ru(1)-P(1)	154.57(10)
C(2)-Ru(1)-P(1)	160.65(10)
C(5)-Ru(1)-Cl(2)	150.26(13)
C(6)-Ru(1)-Cl(2)	112.63(12)
C(4)-Ru(1)-Cl(2)	160.19(10)
C(1)-Ru(1)-Cl(2)	89.00(11)
C(3)-Ru(1)-Cl(2)	122.60(10)

C(2)-Ru(1)-Cl(2)	94.81(10)
P(1)-Ru(1)-Cl(2)	82.45(3)
C(5)-Ru(1)-Cl(1)	120.70(13)
C(6)-Ru(1)-Cl(1)	158.49(12)
C(4)-Ru(1)-Cl(1)	91.16(11)
C(1)-Ru(1)-Cl(1)	148.19(11)
C(3)-Ru(1)-Cl(1)	88.36(11)
C(2)-Ru(1)-Cl(1)	111.31(10)
P(1)-Ru(1)-Cl(1)	87.85(3)
Cl(2)-Ru(1)-Cl(1)	88.78(3)
C(17)-P(1)-C(11)	105.06(16)
C(17)-P(1)-C(23)	105.44(16)
C(11)-P(1)-C(23)	103.22(16)
C(17)-P(1)-Ru(1)	112.73(11)
C(11)-P(1)-Ru(1)	115.37(11)
C(23)-P(1)-Ru(1)	113.95(11)
C(24)-P(2)-C(30)	102.57(17)
C(24)-P(2)-C(23)	103.30(16)
C(30)-P(2)-C(23)	99.54(15)
C(6)-C(1)-C(2)	118.1(4)
C(6)-C(1)-C(7)	123.5(4)
C(2)-C(1)-C(7)	118.3(4)
C(6)-C(1)-Ru(1)	70.3(2)
C(2)-C(1)-Ru(1)	72.5(2)
C(7)-C(1)-Ru(1)	131.1(3)
C(3)-C(2)-C(1)	120.9(4)
C(3)-C(2)-Ru(1)	71.8(2)
C(1)-C(2)-Ru(1)	70.1(2)
C(3)-C(2)-H(2)	119.5
C(1)-C(2)-H(2)	119.5
Ru(1)-C(2)-H(2)	131.4
C(2)-C(3)-C(4)	121.8(4)
C(2)-C(3)-Ru(1)	72.5(2)
C(4)-C(3)-Ru(1)	70.3(2)
C(2)-C(3)-H(3)	119.1
C(4)-C(3)-H(3)	119.1
Ru(1)-C(3)-H(3)	131.0
C(5)-C(4)-C(3)	117.4(4)

C(5)-C(4)-C(10)	122.4(4)
C(3)-C(4)-C(10)	120.2(4)
C(5)-C(4)-Ru(1)	69.7(2)
C(3)-C(4)-Ru(1)	72.1(2)
C(10)-C(4)-Ru(1)	130.3(3)
C(4)-C(5)-C(6)	121.2(4)
C(4)-C(5)-Ru(1)	73.0(2)
C(6)-C(5)-Ru(1)	71.6(2)
C(4)-C(5)-H(5)	119.4
C(6)-C(5)-H(5)	119.4
Ru(1)-C(5)-H(5)	128.3
C(1)-C(6)-C(5)	120.4(4)
C(1)-C(6)-Ru(1)	72.4(2)
C(5)-C(6)-Ru(1)	70.3(2)
C(1)-C(6)-H(6)	119.8
C(5)-C(6)-H(6)	119.8
Ru(1)-C(6)-H(6)	130.1
C(1)-C(7)-C(9)	115.3(4)
C(1)-C(7)-C(8)	108.0(4)
C(9)-C(7)-C(8)	112.3(5)
C(1)-C(7)-H(7)	110(3)
C(9)-C(7)-H(7)	102(3)
C(8)-C(7)-H(7)	109(3)
C(7)-C(8)-H(8A)	109.5
C(7)-C(8)-H(8B)	109.5
H(8A)-C(8)-H(8B)	109.5
C(7)-C(8)-H(8C)	109.5
H(8A)-C(8)-H(8C)	109.5
H(8B)-C(8)-H(8C)	109.5
C(7)-C(9)-H(9A)	109.5
C(7)-C(9)-H(9B)	109.5
H(9A)-C(9)-H(9B)	109.5
C(7)-C(9)-H(9C)	109.5
H(9A)-C(9)-H(9C)	109.5
H(9B)-C(9)-H(9C)	109.5
C(4)-C(10)-H(10A)	109.5
C(4)-C(10)-H(10B)	109.5
H(10A)-C(10)-H(10B)	109.5

C(4)-C(10)-H(10C)	109.5
H(10A)-C(10)-H(10C)	109.5
H(10B)-C(10)-H(10C)	109.5
C(12)-C(11)-C(16)	118.3(3)
C(12)-C(11)-P(1)	117.7(3)
C(16)-C(11)-P(1)	123.7(3)
C(11)-C(12)-C(13)	120.6(4)
C(11)-C(12)-H(12)	119.7
C(13)-C(12)-H(12)	119.7
C(14)-C(13)-C(12)	119.8(5)
C(14)-C(13)-H(13)	120.1
C(12)-C(13)-H(13)	120.1
C(15)-C(14)-C(13)	120.3(4)
C(15)-C(14)-H(14)	119.8
C(13)-C(14)-H(14)	119.8
C(14)-C(15)-C(16)	120.4(4)
C(14)-C(15)-H(15)	119.8
C(16)-C(15)-H(15)	119.8
C(15)-C(16)-C(11)	120.5(4)
C(15)-C(16)-H(16)	119.7
C(11)-C(16)-H(16)	119.7
C(22)-C(17)-C(18)	118.1(4)
C(22)-C(17)-P(1)	121.3(3)
C(18)-C(17)-P(1)	120.3(3)
C(19)-C(18)-C(17)	120.6(5)
C(19)-C(18)-H(18)	119.7
C(17)-C(18)-H(18)	119.7
C(20)-C(19)-C(18)	121.0(5)
C(20)-C(19)-H(19)	119.5
C(18)-C(19)-H(19)	119.5
C(21)-C(20)-C(19)	118.9(5)
C(21)-C(20)-H(20)	120.6
C(19)-C(20)-H(20)	120.6
C(20)-C(21)-C(22)	120.9(5)
C(20)-C(21)-H(21)	119.5
C(22)-C(21)-H(21)	119.5
C(17)-C(22)-C(21)	120.5(5)
C(17)-C(22)-H(22)	119.7

C(21)-C(22)-H(22)	119.7
P(1)-C(23)-P(2)	114.74(17)
P(1)-C(23)-H(23A)	108.6
P(2)-C(23)-H(23A)	108.6
P(1)-C(23)-H(23B)	108.6
P(2)-C(23)-H(23B)	108.6
H(23A)-C(23)-H(23B)	107.6
C(25)-C(24)-C(29)	117.7(4)
C(25)-C(24)-P(2)	126.0(3)
C(29)-C(24)-P(2)	116.3(3)
C(26)-C(25)-C(24)	121.0(5)
C(26)-C(25)-H(25)	119.5
C(24)-C(25)-H(25)	119.5
C(27)-C(26)-C(25)	120.7(5)
C(27)-C(26)-H(26)	119.6
C(25)-C(26)-H(26)	119.6
C(26)-C(27)-C(28)	120.0(5)
C(26)-C(27)-H(27)	120.0
C(28)-C(27)-H(27)	120.0
C(27)-C(28)-C(29)	119.7(5)
C(27)-C(28)-H(28)	120.1
C(29)-C(28)-H(28)	120.1
C(24)-C(29)-C(28)	120.8(4)
C(24)-C(29)-H(29)	119.6
C(28)-C(29)-H(29)	119.6
C(35)-C(30)-C(31)	117.5(4)
C(35)-C(30)-P(2)	116.8(3)
C(31)-C(30)-P(2)	125.6(3)
C(30)-C(31)-C(32)	120.8(4)
C(30)-C(31)-H(31)	119.6
C(32)-C(31)-H(31)	119.6
C(33)-C(32)-C(31)	120.8(5)
C(33)-C(32)-H(32)	119.6
C(31)-C(32)-H(32)	119.6
C(32)-C(33)-C(34)	119.8(5)
C(32)-C(33)-H(33)	120.1
C(34)-C(33)-H(33)	120.1
C(33)-C(34)-C(35)	120.2(5)

C(33)-C(34)-H(34)	119.9
C(35)-C(34)-H(34)	119.9
C(30)-C(35)-C(34)	120.8(4)
C(30)-C(35)-H(35)	119.6
C(34)-C(35)-H(35)	119.6

Symmetry transformations used to generate equivalent atoms:

Table 4. Anisotropic displacement parameters ($Å^2$x 10^3)for rudppm. The anisotropic displacement factor exponent takes the form: $-2\pi^2[h^2a^{*2}U^{11} + ... + 2 h k a^* b^* U^{12}]$

	U^{11}	U^{22}	U^{33}	U^{23}	U^{13}	U^{12}
Ru(1)	30(1)	32(1)	26(1)	-8(1)	-1(1)	-2(1)
Cl(1)	42(1)	49(1)	52(1)	-16(1)	0(1)	-16(1)
Cl(2)	45(1)	47(1)	29(1)	0(1)	-1(1)	-4(1)
P(1)	30(1)	29(1)	26(1)	-6(1)	-2(1)	-2(1)
P(2)	30(1)	36(1)	35(1)	-9(1)	-3(1)	-2(1)
C(1)	24(2)	45(2)	62(2)	-12(2)	-1(2)	5(2)
C(2)	37(2)	45(2)	41(2)	-14(2)	2(2)	4(2)
C(3)	48(2)	32(2)	45(2)	-11(2)	-2(2)	4(2)
C(4)	51(2)	38(2)	37(2)	-1(2)	-6(2)	9(2)
C(5)	50(2)	54(2)	37(2)	-11(2)	-15(2)	13(2)
C(6)	32(2)	50(2)	66(3)	-25(2)	-21(2)	9(2)
C(7)	40(3)	59(3)	95(4)	-14(3)	14(3)	-8(2)
C(8)	45(3)	91(4)	233(9)	-30(5)	49(4)	-6(3)
C(9)	63(3)	72(3)	139(5)	-20(3)	18(3)	-31(3)
C(10)	91(4)	48(3)	55(3)	8(2)	8(2)	5(2)
C(11)	35(2)	37(2)	31(2)	-5(2)	-2(1)	3(2)
C(12)	70(3)	38(2)	44(2)	-6(2)	14(2)	-4(2)
C(13)	95(4)	53(3)	61(3)	11(2)	28(3)	-7(3)
C(14)	79(4)	83(4)	38(2)	6(2)	15(2)	11(3)
C(15)	59(3)	85(3)	37(2)	-23(2)	-1(2)	6(2)
C(16)	42(2)	52(2)	38(2)	-15(2)	-2(2)	1(2)
C(17)	35(2)	37(2)	41(2)	-12(2)	-1(2)	-7(2)
C(18)	47(3)	54(3)	64(3)	-17(2)	-9(2)	-13(2)
C(19)	61(3)	81(4)	101(4)	-38(3)	-15(3)	-25(3)
C(20)	71(4)	71(4)	126(5)	-32(3)	8(3)	-40(3)
C(21)	98(4)	52(3)	104(4)	2(3)	0(3)	-33(3)
C(22)	62(3)	45(2)	67(3)	0(2)	-6(2)	-19(2)
C(23)	30(2)	38(2)	31(2)	-5(2)	-2(1)	-3(2)
C(24)	34(2)	43(2)	42(2)	-5(2)	0(2)	-5(2)
C(25)	82(4)	67(3)	73(3)	-22(2)	27(3)	-39(3)
C(26)	116(5)	83(4)	121(5)	-31(4)	41(4)	-62(4)
C(27)	107(5)	104(5)	115(5)	-9(4)	43(4)	-68(4)
C(28)	80(4)	105(4)	69(3)	-12(3)	28(3)	-36(3)

C(29)	52(3)	65(3)	51(2)	-8(2)	9(2)	-11(2)
C(30)	32(2)	37(2)	41(2)	-7(2)	1(2)	2(2)
C(31)	57(3)	57(3)	61(3)	-2(2)	-22(2)	-13(2)
C(32)	71(4)	86(4)	68(3)	-3(3)	-33(3)	-6(3)
C(33)	59(3)	79(3)	54(3)	4(2)	-10(2)	15(3)
C(34)	78(4)	61(3)	95(4)	31(3)	-14(3)	-9(3)
C(35)	51(3)	57(3)	83(3)	14(2)	-16(2)	-16(2)

Table 5. Hydrogen coordinates (x 10^4) and isotropic displacement parameters ($Å^2$x 10^3) for rudppm.

	x	y	z	U(eq)
H(2)	-1375	5313	4562	52
H(3)	-295	6392	3433	52
H(5)	-356	4442	1033	60
H(6)	-1496	3352	2175	60
H(7)	-1930(40)	3360(40)	4930(30)	55(14)
H(8A)	-3511	5051	4567	194
H(8B)	-3966	3943	5057	194
H(8C)	-3933	4281	3831	194
H(9A)	-2561	2316	3361	136
H(9B)	-2674	1905	4575	136
H(9C)	-1405	1824	3945	136
H(10A)	1182	6357	1730	106
H(10B)	22	7015	1203	106
H(10C)	845	5876	737	106
H(12)	2445	4114	1083	65
H(13)	3310	4501	-617	91
H(14)	3465	3212	-1892	90
H(15)	2861	1511	-1467	76
H(16)	2045	1084	229	55
H(18)	-101	1814	952	65
H(19)	-1235	457	1028	92
H(20)	-1047	-1077	2324	102
H(21)	309	-1251	3539	100
H(22)	1448	109	3487	69
H(23A)	2776	1081	3463	41
H(23B)	3316	2157	3043	41
H(25)	4724	2826	2403	87
H(26)	5970	3939	1545	123
H(27)	7046	3440	-38	127
H(28)	6987	1738	-727	102
H(29)	5735	594	127	69
H(31)	6165	677	3154	69

H(32)	7269	-631	4340	90
H(33)	6811	-2372	4885	84
H(34)	5254	-2850	4253	98
H(35)	4147	-1570	3033	77

Table 6. Torsion angles [°] for rudppm.

C(6)-C(1)-C(2)-C(3)	-2.4(5)
C(7)-C(1)-C(2)-C(3)	-179.3(4)
Ru(1)-C(1)-C(2)-C(3)	52.9(3)
C(6)-C(1)-C(2)-Ru(1)	-55.3(3)
C(7)-C(1)-C(2)-Ru(1)	127.8(4)
C(1)-C(2)-C(3)-C(4)	0.1(6)
Ru(1)-C(2)-C(3)-C(4)	52.3(3)
C(1)-C(2)-C(3)-Ru(1)	-52.1(3)
C(2)-C(3)-C(4)-C(5)	1.5(5)
Ru(1)-C(3)-C(4)-C(5)	54.7(3)
C(2)-C(3)-C(4)-C(10)	180.0(4)
Ru(1)-C(3)-C(4)-C(10)	-126.8(4)
C(2)-C(3)-C(4)-Ru(1)	-53.2(3)
C(3)-C(4)-C(5)-C(6)	-0.8(5)
C(10)-C(4)-C(5)-C(6)	-179.3(4)
Ru(1)-C(4)-C(5)-C(6)	55.1(3)
C(3)-C(4)-C(5)-Ru(1)	-55.9(3)
C(10)-C(4)-C(5)-Ru(1)	125.6(4)
C(2)-C(1)-C(6)-C(5)	3.0(5)
C(7)-C(1)-C(6)-C(5)	179.7(4)
Ru(1)-C(1)-C(6)-C(5)	-53.3(3)
C(2)-C(1)-C(6)-Ru(1)	56.3(3)
C(7)-C(1)-C(6)-Ru(1)	-126.9(4)
C(4)-C(5)-C(6)-C(1)	-1.4(6)
Ru(1)-C(5)-C(6)-C(1)	54.3(3)
C(4)-C(5)-C(6)-Ru(1)	-55.8(3)
C(6)-C(1)-C(7)-C(9)	24.8(7)
C(2)-C(1)-C(7)-C(9)	-158.5(4)
Ru(1)-C(1)-C(7)-C(9)	-67.6(6)
C(6)-C(1)-C(7)-C(8)	-101.7(5)
C(2)-C(1)-C(7)-C(8)	75.0(6)
Ru(1)-C(1)-C(7)-C(8)	165.9(4)
C(17)-P(1)-C(11)-C(12)	165.5(3)
C(23)-P(1)-C(11)-C(12)	-84.3(3)
Ru(1)-P(1)-C(11)-C(12)	40.7(3)
C(17)-P(1)-C(11)-C(16)	-21.6(3)

C(23)-P(1)-C(11)-C(16)	88.6(3)
Ru(1)-P(1)-C(11)-C(16)	-146.4(3)
C(16)-C(11)-C(12)-C(13)	1.1(6)
P(1)-C(11)-C(12)-C(13)	174.4(4)
C(11)-C(12)-C(13)-C(14)	0.8(7)
C(12)-C(13)-C(14)-C(15)	-1.8(8)
C(13)-C(14)-C(15)-C(16)	0.9(7)
C(14)-C(15)-C(16)-C(11)	1.0(6)
C(12)-C(11)-C(16)-C(15)	-2.0(6)
P(1)-C(11)-C(16)-C(15)	-174.9(3)
C(11)-P(1)-C(17)-C(22)	139.3(3)
C(23)-P(1)-C(17)-C(22)	30.6(3)
Ru(1)-P(1)-C(17)-C(22)	-94.3(3)
C(11)-P(1)-C(17)-C(18)	-46.6(3)
C(23)-P(1)-C(17)-C(18)	-155.3(3)
Ru(1)-P(1)-C(17)-C(18)	79.8(3)
C(22)-C(17)-C(18)-C(19)	0.0(6)
P(1)-C(17)-C(18)-C(19)	-174.2(3)
C(17)-C(18)-C(19)-C(20)	0.0(7)
C(18)-C(19)-C(20)-C(21)	-0.3(8)
C(19)-C(20)-C(21)-C(22)	0.5(9)
C(18)-C(17)-C(22)-C(21)	0.2(6)
P(1)-C(17)-C(22)-C(21)	174.4(4)
C(20)-C(21)-C(22)-C(17)	-0.5(8)
C(17)-P(1)-C(23)-P(2)	74.9(2)
C(11)-P(1)-C(23)-P(2)	-35.1(2)
Ru(1)-P(1)-C(23)-P(2)	-160.98(13)
C(24)-P(2)-C(23)-P(1)	94.8(2)
C(30)-P(2)-C(23)-P(1)	-159.7(2)
C(30)-P(2)-C(24)-C(25)	-82.3(4)
C(23)-P(2)-C(24)-C(25)	20.9(4)
C(30)-P(2)-C(24)-C(29)	98.6(3)
C(23)-P(2)-C(24)-C(29)	-158.3(3)
C(29)-C(24)-C(25)-C(26)	-0.1(8)
P(2)-C(24)-C(25)-C(26)	-179.3(5)
C(24)-C(25)-C(26)-C(27)	1.1(11)
C(25)-C(26)-C(27)-C(28)	-2.2(12)
C(26)-C(27)-C(28)-C(29)	2.1(11)

C(25)-C(24)-C(29)-C(28)	0.1(7)
P(2)-C(24)-C(29)-C(28)	179.3(4)
C(27)-C(28)-C(29)-C(24)	-1.1(9)
C(24)-P(2)-C(30)-C(35)	-158.4(3)
C(23)-P(2)-C(30)-C(35)	95.5(3)
C(24)-P(2)-C(30)-C(31)	17.9(4)
C(23)-P(2)-C(30)-C(31)	-88.1(4)
C(35)-C(30)-C(31)-C(32)	0.2(6)
P(2)-C(30)-C(31)-C(32)	-176.2(4)
C(30)-C(31)-C(32)-C(33)	-0.5(8)
C(31)-C(32)-C(33)-C(34)	0.2(8)
C(32)-C(33)-C(34)-C(35)	0.4(8)
C(31)-C(30)-C(35)-C(34)	0.5(7)
P(2)-C(30)-C(35)-C(34)	177.1(4)
C(33)-C(34)-C(35)-C(30)	-0.8(8)

Symmetry transformations used to generate equivalent atoms:

Table 7. Hydrogen bonds for rudppm [and].

D-H...A	d(D-H)	d(H...A)	d(D...A)	<(DHA)
C(23)-H(23B)...Cl(1)	0.97	2.68	3.380(4)	128.9
C(12)-H(12)...Cl(1)	0.93	2.86	3.663(4)	145.9
C(2)-H(2)...Cl(1)#1	0.93	2.81	3.725(4)	170.0
C(3)-H(3)...Cl(2)#1	0.93	0.81	3.529(4)	135.0

Symmetry transformations used to generate equivalent atoms: #1 -x,-y+1,-z+1

Supplementary data

Characterization of [Ru(*p*-cymene)(dppm)Cl_2] complex

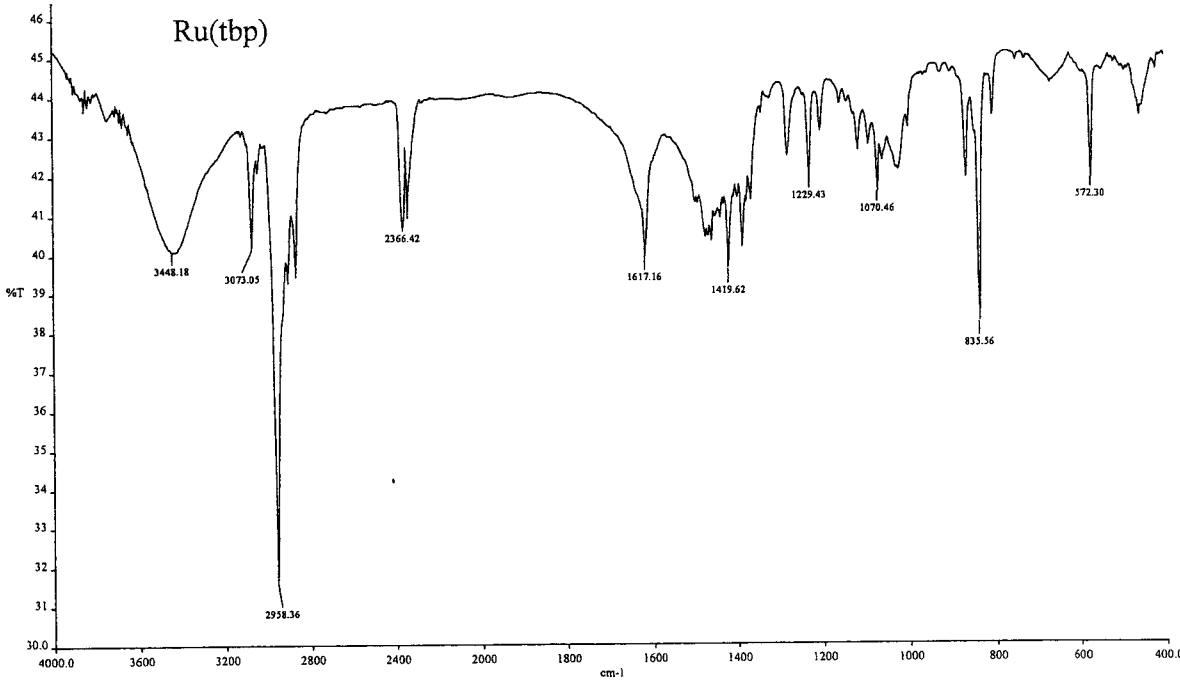

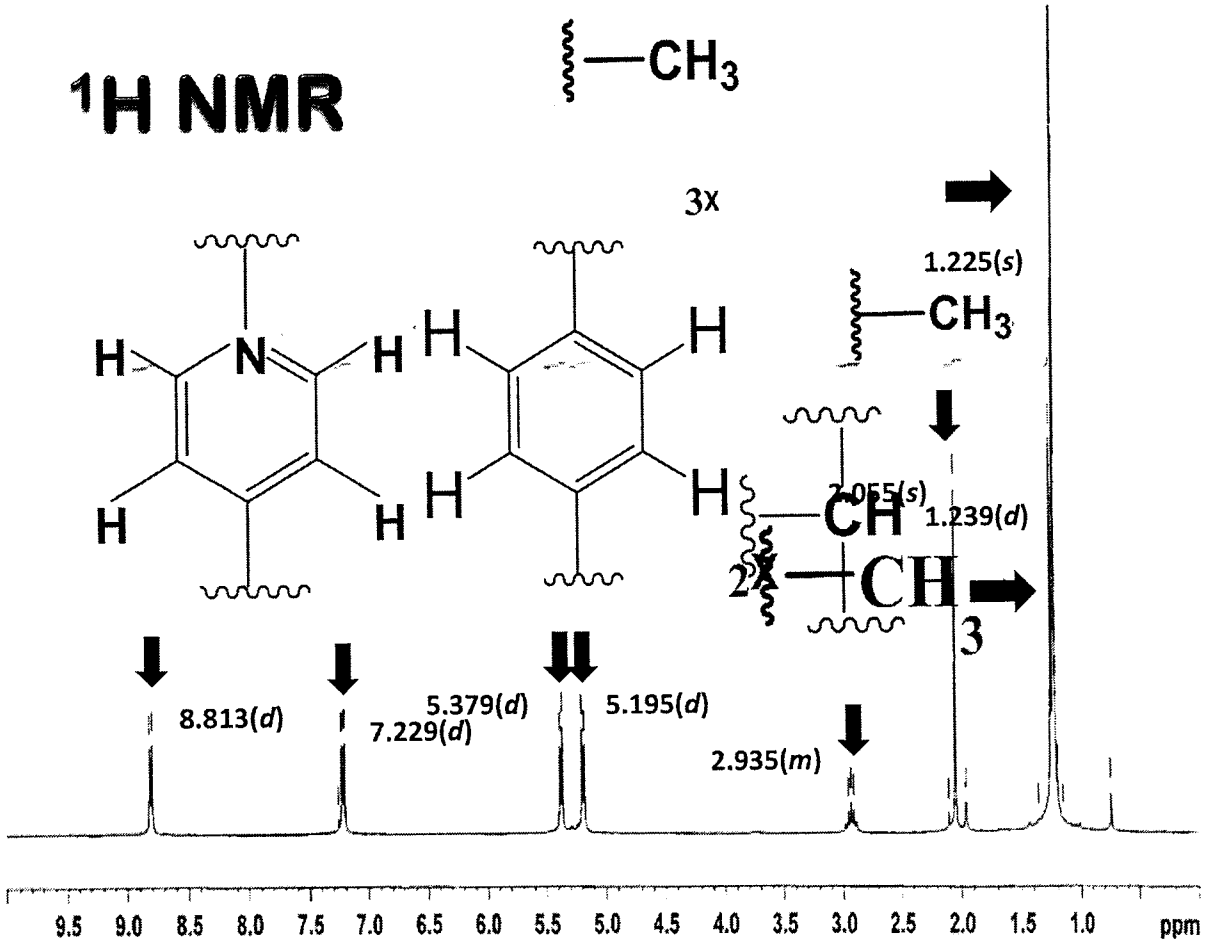
1H NMR
—CH3
3x
1.225(s)
—CH3
2.055(s)
1.239(d)
2x
—CH
—CH3
8.813(d)
7.229(d)
5.379(d)
5.195(d)
2.935(m)
9.5 9.0 8.5 8.0 7.5 7.0 6.5 6.0 5.5 5.0 4.5 4.0 3.5 3.0 2.5 2.0 1.5 1.0
ppm

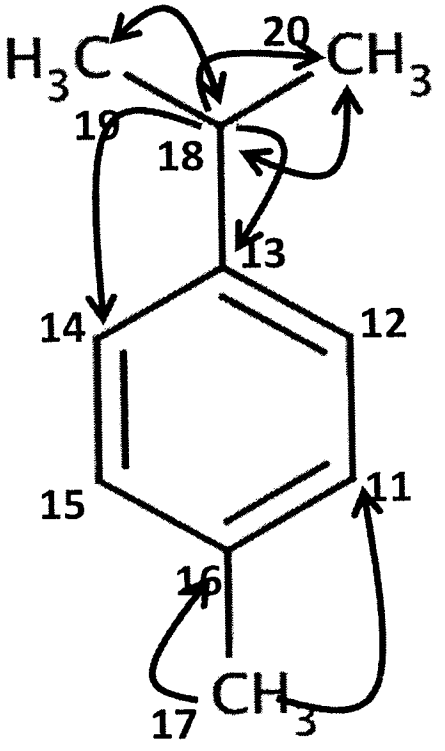

COSY

HMBC

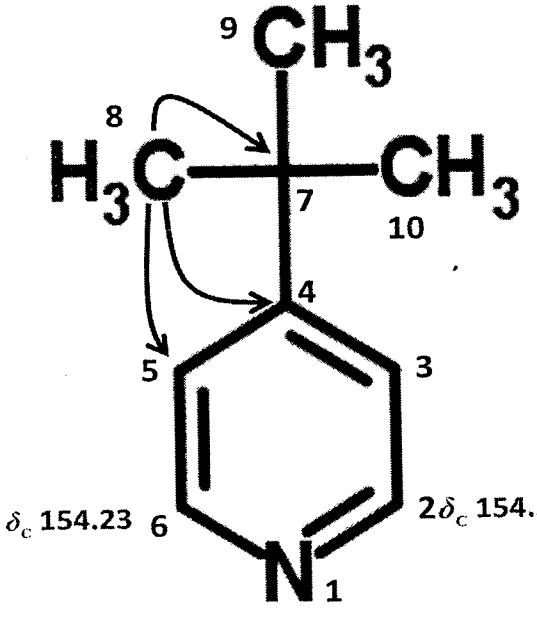

COSY

HMBC

Complex	Elemental analysis (%)					
	Calculated			Found		
	C	H	N	C	H	N
Ru(tbp)	51.70	6.17	3.17	51.48±0.16	6.28±0.05	3.13±0.09